Biogeochemistry (2026) 169:47
https://doi.org/10.1007/s10533-026-01343-x

Integrating field, mesocosms, and laboratory approaches to characterise denitrification-driven nitrous oxide hot moments in European wetlands

Thomas Crestey-Chury · Romain Darnajoux · Sabine Sauvage · Mika Aurela · Thierry Camboulive · Noémie Carles · Tom De Dobbelaer · Laura Escarmena · Laure Gandois · Jyrki Jauhiainen · Sari Juutinen · Tuula Larmola · Ülo Mander · Sílvia Poblador · Maud Raman · Francesc Sabater · Thomas Schindler · Kaido Soosaar · Liisa Ukonmaanaho · José-Miguel Sánchez-Pérez

Received: 14 November 2025 / Accepted: 5 May 2026
© The Author(s) 2026

Abstract A substantial part of terrestrial nitrous oxide (N_2O) emissions originates from denitrification in wetlands, and this contribution is expected to rise with ongoing land-use changes, such as wetland drainage, agricultural conversion, and peatland degradation, as well as under global warming. Capturing the spatial and temporal dynamics of N_2O emissions through measurements and numerical modelling remains challenging, as extreme N_2O peaks occur during short-lived transient events (hot moments). In this study, we combined three experimental approaches (in situ field monitoring, mesocosm experiments, and slurry soil incubations in the laboratory) to characterise N_2O hot moments of denitrification across 21 diverse European wetlands. Each approach captured different aspects of N_2O emission dynamics, and their combination revealed additional features, including the timing and magnitude of N_2O fluxes, denitrification efficiency (ratio of N_2O to N_2O+N_2 emitted), and an estimate of the proportion of soil actively undergoing denitrification. We encourage the use of these key determinants to improve and parametrise future denitrification models that aim to quantify transient N_2O hot moments.

Keywords Wetland · Denitrification · Nitrous oxide · Hot moment · Mesocosm · DEA

Introduction

Nitrous oxide (N_2O), together with carbon dioxide (CO_2) and methane (CH_4), is one of the three major greenhouse gases (GHG). Despite its lower

Supplementary Information The online version contains supplementary material available at https://doi.org/10.1007/s10533-026-01343-x.

Responsible Editor: Klaus-Holger Knorr.

T. Crestey-Chury (✉) · R. Darnajoux · S. Sauvage · T. Camboulive · N. Carles · L. Gandois · J.-M. Sánchez-Pérez
Centre de Recherche sur la Biodiversité et l'environnement (CRBE), Université de Toulouse, CNRS, IRD, Toulouse INP, Toulouse, France
e-mail: tcrestey@insa-toulouse.fr

M. Aurela · S. Juutinen
Finnish Meteorological Institute, Helsinki, Finland

T. De Dobbelaer · M. Raman
Research Institute Nature and Forest (INBO), Brussels, Belgium

L. Escarmena · S. Poblador · F. Sabater
Departement de Biologia Evolutiva, Ecologia i Ciències Ambientals, Facultat de Biologia, Universitat de Barcelona, Barcelona, Spain

J. Jauhiainen · T. Larmola · L. Ukonmaanaho
Natural Resources Institute Finland (Luke), Helsinki, Finland

Ü. Mander · T. Schindler · K. Soosaar
University of Tartu, Tartu, Estonia

S. Poblador · F. Sabater
CREAF, Cerdanyola del Vallès, Barcelona, Spain

Published online: 22 May 2026

atmospheric concentration, N_2O has a global warming potential 273 times higher than CO_2 (IPCC Sixth Assessment Report, 2023). It is also projected to become the dominant ozone-depleting substance of the twenty-first century if emissions remain unchecked (Ravishankara et al. 2009). As global terrestrial N_2O emissions are expected to rise from 11 Tg N yr^{-1} in 2020 to 16 Tg N yr^{-1} by 2100 (De Sisto et al. 2024), understanding the underlying mechanisms driving these emissions is crucial to mitigate them. Natural soils are the largest global source of N_2O emissions, estimated at 6.4 (3.9–8.6) Tg N yr^{-1}, comparable to all anthropogenic sources combined (Tian et al. 2024). Among natural soils, wetlands are the most important N_2O emitters, especially peatlands (Pärn et al. 2018) and riparian forests (Mander et al. 2021; Christensen & Rousk 2024). A substantial part of their high annual emissions may be associated with environmental perturbations such as frequent hydrological flooding events (Jørgensen & Elberling 2012), or anthropogenic disturbances such as drainage, forestation (Hernandez & Mitsch 2006) or restoration (Klionsky et al. 2024). Due to their sensitivity to these environmental and anthropogenic changes, wetlands are a particularly relevant system for studying increasing N_2O emissions. Understanding the extent to which these changes influence wetlands N_2O emissions is therefore important for developing mitigation strategies.

Multiple microbial pathways contribute to N_2O production, depending on local environmental conditions. Under anoxic conditions, N_2O can arise as an intermediate of heterotrophic bacterial denitrification or during incomplete dissimilatory nitrate reduction to ammonium (DNRA), a process that remains poorly understood (Schreiber et al. 2012; Xu et al. 2024). Under aerobic conditions, ammonia-oxidising bacteria and archaea produce N_2O either through incomplete oxidation of ammonium to nitrite during nitrification, or via nitrifier denitrification, in which N_2O is formed through pathways analogous to heterotrophic denitrification. These processes coexist in wetlands, with their relative contributions shaped by oxygen availability, organic carbon levels, and nitrate supply. In aerobic drained wetlands, archaeal nitrification may predominate N_2O emissions (Bahram et al. 2022), while rewetted sites tend to favour denitrification, with additional contributions from DNRA and nitrification (Masta et al. 2022). High nitrate levels under anaerobic conditions further enhance denitrification (Wrage et al. 2004), and the carbon-to-nitrate ratio often determines whether denitrification or DNRA is dominant (Hardison et al. 2015; van den Berg et al. 2016; Hernández-del Amo and Bañeras 2021), with a low ratio leading to predominance of denitrification. The intensification of freeze–thaw and wet-dry cycles due to global warming (Guo et al. 2014; Congreves et al. 2018), combined with sustained nitrate inputs from agriculture (Lind et al. 2013), is expected to amplify N_2O release through denitrification.

Denitrification is a four-step anaerobic respiratory pathway performed by facultative heterotrophic bacteria, in which nitrate (NO_3^-) is sequentially reduced to nitrite (NO_2^-), nitric oxide (NO), N_2O, and finally dinitrogen (N_2). The process relies on organic carbon as an electron donor, and is therefore closely linked to heterotrophic respiration, which simultaneously produces CO_2, further contributing to soil greenhouse gas emissions. As N_2O is an intermediate in this pathway, its emission occurs when denitrification is incomplete (Knowles 1982). During incomplete denitrification, N_2O emission peaks typically occur during short-lived events referred to as *hot moments*, and only in specific soil volumes that provide ideal conditions for denitrifier bacteria, called *hotspots* (Zhao et al. 2021). Denitrification hotspots are governed by a combination of physical controls (optimal soil temperature, anoxic conditions), chemical controls (nitrate and carbon availability), and biological controls (abundance and activity of denitrifiers) (Chen et al. 2018). These conditions are rarely met uniformly throughout the soil profile but instead occur within small, cm- to mm-scale patches defined by soil structure and porosity, often referred to as microsites (Schlüter et al. 2025). A denitrification hot moment can only occur when all these conditions are met.

A hot moment is defined as a high rate of N_2O emissions compared to baseline levels over longer periods, and lasting only for a short time (Groffman 2012). To date, no universally accepted threshold for identifying denitrification-driven N_2O hot moments exists, partly explained by the fact that N_2O can be emitted by other microbial pathways such as nitrification or DNRA. Stuchiner et al. (2025) proposed defining N_2O hot moments as emissions exceeding 1.5 times the interquartile range of annual fluxes, based on continuous measurements in an agricultural soil.

Ackett et al. (2025) evaluated the efficiency of this method as well as 13 others to discriminate N_2O hot moments in agricultural soils and concluded that the most effective methods were based on median absolute deviation and minimum covariance determinant. While promising, these approaches are generally derived from total N_2O fluxes and do not distinguish among the different microbial pathways contributing to N_2O production. Because the relative contribution of these pathways varies across environmental conditions and ecosystem types, no universal threshold can be readily applied to identify denitrification-driven N_2O hot moments. In addition, they may be difficult to apply to short-term or intraday field studies and may not be widely applicable across ecosystems. Because hot moments depend on site-specific environmental constraints and the relative contribution of each N_2O-producing microbial pathway, thresholds derived from a single soil type risk under- or overestimating their occurrence in natural systems such as wetlands.

Hot moments are inherently difficult to quantify, as their prediction requires identifying when and where all environmental controls converge to form an active hotspot. Despite the development of various numerical models to simulate N_2O emissions attributable to denitrification (Heinen 2006), only a limited number explicitly incorporate hotspots and hot moments, even though these events may account for a substantial fraction of total N_2O emissions (Groffman et al. 2009). Moreover, the reliability of these models is heavily dependent on robust empirical parameters (Martínez-Espinosa et al. 2021), which must be calibrated across a wide range of sites to encompass the large variability inherent to these processes (Boyer et al. 2006; Groffman et al. 2009). Among the environmental parameters influencing N_2O hot moments, soil water content is the most commonly and easily measured, serving as the best proxy for soil oxygen availability (Butterbach-Bahl et al. 2013). Its relationship with N_2O flux is nonlinear and unimodal, reflecting the interaction of the two primary N_2O-producing processes: nitrification (aerobic and suboxic) and denitrification (suboxic and anaerobic) (Davidson and Verchot 2000; Pärn et al. 2018; Mander et al. 2021). Traditionally, hot moments have been predicted based on the frequency of soil freeze–thaw cycles (Wagner-Riddle et al. 2017; Kazmi et al. 2025) and abrupt changes in soil water content (e.g., groundwater table fluctuations; Anthony and Silver 2021; Mander et al. 2021). Changes in topsoil water content also play a critical role in freeze–thaw cycles (Öquist et al. 2004; Kazmi et al. 2025). Other critical parameters include nitrate and carbon availability, and soil temperature (Heinen 2006). These parameters are typically acquired through field measurements, mesocosm studies, or slurry incubations (Butterbach-Bahl et al. 2013).

Field measurements are regarded as the most ecologically relevant, as they capture N_2O emissions in unchanged soil conditions (Groffman et al. 2006). However, heterogeneous water flow, soil microtopography, and preferential pathways may limit nitrate availability and impede the occurrence of fully anaerobic zones required for the formation of denitrification hotspots. As a result, alternative N_2O-producing processes such as nitrification, nitrifier denitrification, or DNRA can be active (Masta et al. 2022). Slurry soil laboratory incubations offer precise control over experimental variables (Khalil et al. 2005). Denitrification enzyme activity (DEA) assays, for example, ensure that denitrification is the dominant process during the experiment, by adding water and nitrate solution while removing all oxic and nitrate-depleted microstructures (Tiedje et al. 1989). Yet, these assays lack ecological realism due to soil structure loss and inhibition of aerobic metabolisms, limiting their ability to reflect the natural dynamics of N_2O hot moments. Intact core experiments offer a middle ground, maintaining semi-controlled conditions while preserving soil structure (Dinsmore et al. 2008; Peng et al. 2019). They allow continuous measurement of N_2O emissions, capturing the full extent of hot moments (Kanaan et al. 2025). Because soil structure remains intact, oxic microsites may persist, thereby enabling aerobic processes such as nitrification and nitrifier denitrification. In addition, the physical structure of the soil can restrict nutrient diffusion, potentially creating nitrate- or carbon-depleted microsites.

In situ, mesocosm and DEA experiments alone are insufficient to characterise all aspects of denitrification-driven N_2O hot moments, and few studies have combined these approaches to obtain a more comprehensive understanding of the process. Van den Heuvel et al. (2009) measured in situ N_2O emissions in a Dutch riparian buffer zone and conducted slurry incubations with acetate or nitrate amendments to explore environmental drivers of transient N_2O emissions in

hotspots. Mander et al. (2014) used both in situ and intact soil cores experiments to track N_2O and N_2 emissions from a riparian forest, as well as the N_2O: ($N_2O + N_2$) ratio. Douglas et al. (2022) combined in situ N_2 flux measurements with DEA assays to characterise total denitrification hot moments in estuaries. While these studies demonstrate the power of combining experimental approaches, neither focused directly on the dynamics of soil N_2O emissions attributable to denitrification. Moreover, all the aforementioned studies were restricted to a limited number of sites and types of ecosystems, constraining inference at broader scales.

In this study, in situ monitoring, mesocosm experiments, and slurry incubations were used in combination across 21 diverse wetland soils to investigate N_2O hot moments driven by denitrification. To induce and maximise denitrification-driven hot moments in all experiments, addition of nitrate and water were used to promote anoxia and provide large substrate availability. These treatments were not intended to simulate realistic nutrient inputs (natural precipitation, flood or natural soil cycling) but rather to force the occurrence of hot moments and maximise their detectability, in order to isolate the contribution of denitrification and characterise the temporal dynamics of denitrification-driven N_2O emissions (including their magnitude, duration, and N_2O: N_2 partitioning). Punctual field experiments were used to test which soils created a N_2O hot moment in response to nitrate addition, and at what magnitude. Mesocosm experiments allowed for continuous monitoring of N_2O emissions, and thus were indispensable to describe the entire dynamics of hot moments, namely the timing and magnitude of emissions as well as the total N_2O emitted. Slurry incubations were intended to alleviate chemical and physical constraints on denitrification (maximising nitrate availability, anoxia, temperature, and soil homogeneity), providing the ideal conditions for creating a maximal potential N_2O hot moment and allowing comparison of the inherent biological activity of each soil. These approaches were applied across a network of ecologically diverse European wetland sites encompassing different pedo-climatic conditions and restoration states, including peatlands, floodplains, and forested systems from Finland to Spain, to ensure applicability at large scales. Through the quantification of determinants such as the magnitude and timing of emissions, efficiency of denitrification, and proportion of active microsites, each approach as well as their combination will help calibrate the dynamics of denitrification-driven N_2O hot moments across contrasting wetland types. We hypothesise that these dynamics will differ between wetland types due to differences in chemical composition (nitrogen and carbon content) and soil structure. The overarching goal is the integration of these key determinants into denitrification models, to improve their capacity to predict N_2O emissions from natural soils under dynamic and changing environmental conditions.

Materials and methods

Study sites & sampling strategy

A total of 21 sites were selected across five European countries (Fig. 1a), as part of the ALFAwetlands European project (https://alfawetlands.eu/, ALFAwetlands Project, 2022). These sites, located in Belgium, Estonia, Finland, France, and Spain, were chosen to represent a broad gradient of latitudes, climates, and wetland types (Appendix Table 1), including peatlands, floodplains, alluvial forests, and drained forested peatlands. Peatlands were divided into two groups: classic open peatlands and mountain peatlands, as they are subject to differing light exposure, temperature, and climatic conditions. Measurement periods at each site were determined based on historical climatic data to ensure maximal soil moisture and optimal temperatures for denitrification (25 °C, after Martínez-Espinosa et al. 2022). Accordingly, field campaigns were scheduled for May 2024 in Spain, June 2024 in France and Belgium, and July 2024 in Finland and Estonia.

Because denitrification is most active under anoxic conditions, experimental plots at each site were selected within the most water-saturated zones while avoiding surface flooding. At each site, two treatments were applied to the soil to test nitrate limitations on denitrifier activity: (i) water only and (ii) water + nitrate solution. Adjacent to the field plots, three intact soil cores (10 cm depth × 10 cm diameter) were collected within a 2 m^2 area for mesocosm experiments, and three homogenised slurry samples (top 10 cm) were taken for laboratory incubations (Fig. 1b).

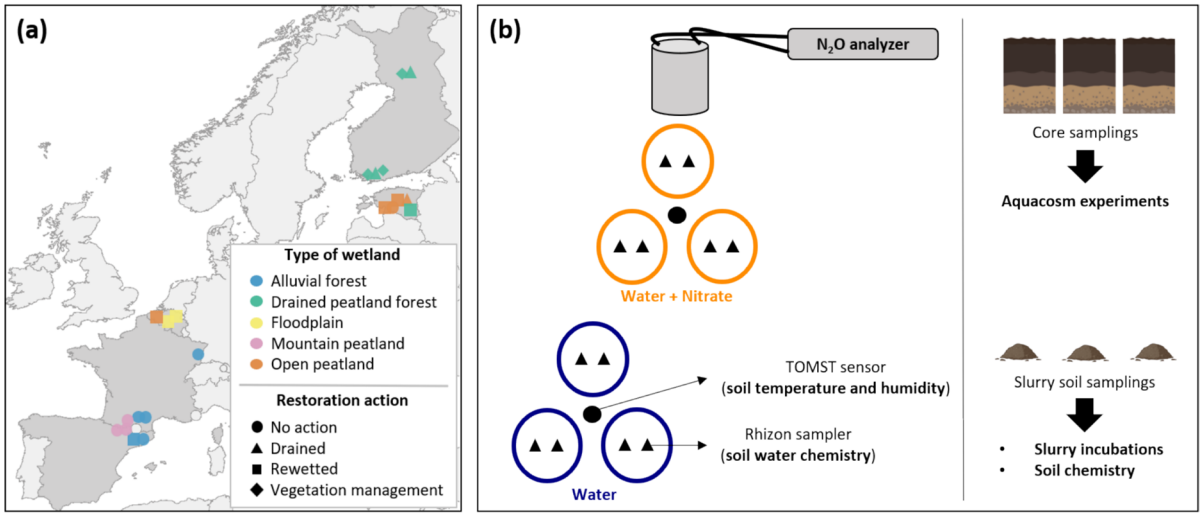

Fig. 1 Description of in situ experiments. Field campaigns were conducted from May to July 2024 to maximise environmental conditions favouring denitrification (high soil moisture and temperature). **a** Location of the study sites across the five countries. Wetland types included natural alluvial forests and mountain peatlands in France and Spain, floodplains and open peatlands in Belgium, open peatlands and drained peatland forests in Estonia, and drained peatland forests in Finland. **b** Schematic of in situ measurements and soil sampling locations within each study site

Field measurements

Six 20 cm-wide plots were established within a 1 m^2 area and divided into two treatment groups with three plots each: control with water only, and water + nitrate. Soil temperature and moisture were recorded continuously using TOMST TMS-4 sensors (TOMST s.r.o., Prague, Czech Republic; Wild et al. 2019), which recorded volumetric water content, soil temperature, surface temperature, and air temperature at one-minute intervals. Two MacroRhizon samplers (Rhizosphere Research Products B.V., Wageningen, The Netherlands) were also installed in each plot to allow pore-water sampling during the experimental period (Fig. 1b). Samples for mesocosm and slurry soil experiments were collected at the end of field measurements.

Treatment solutions were prepared from local groundwater or nearby surface water. For each site, 1 L of untreated water served as the control (solution 1), and 1 L of water containing 100 mg N L^{-1} potassium nitrate (KNO_3; RECTAPUR grade, purity ≥ 98%; purchased from Prolabo, Paris, Île-de-France, France; manufactured in the European Economic Community) was used for the nitrate treatment (solution 2). After initial baseline measurements, 33 cL of each solution was applied to the corresponding plots (solution 1 to plots 1–3; solution 2 to plots 4–6), resulting in a water application equivalent of 10.5 mm and a nitrate application of 4.20 g N m^{-2}. This addition provided excess nitrate to minimise substrate constraints on denitrification, thereby facilitating the isolation of denitrification-driven N_2O emissions. Water addition created transient anaerobic conditions, while nitrate addition further stimulated denitrifying microbial activity. Gas concentrations were monitored using a static chamber system immediately before treatment application, continuously for 2–4 h after addition, and again the following day when site access permitted.

A custom 3D-printed static chamber was used to measure GHG emissions in situ. This chamber was equipped with sensors to monitor internal temperature and pressure, and included a fan to ensure air mixing and homogeneous gas distribution. The chamber was connected via plastic tubing to a LI-COR gas analyser (LI-7820 N_2O/H_2O Trace Gas Analyser from LI-COR Biosciences, Lincoln, NE, USA). During operation, the chamber was sealed to the soil surface, and gas concentrations were recorded for 5 min. Flux rates were derived from the slope of concentration change over time, initially expressed in ppb s^{-1}. Slopes were computed by linear regression in a custom R script, with manual adjustment of time windows to exclude

anomalies. These slopes were converted to N_2O fluxes in µmol m^{-3} h^{-1} using Eq. (1).

$$N_2O \text{ volumetric flux} = N_2O \text{ partial pressure change} \times \frac{PV}{RT} \times \frac{1}{\text{surface} \times \text{depth} \times \text{porosity}} \times 3600 \times 10^{-3} \quad (1)$$

In this equation, the change in N_2O partial pressure is measured in ppb s^{-1} by the analyser. P represent ambient pressure (Pa), T is air temperature (K), V is the chamber and tubing volume (m^3), and R the ideal gas constant (Pa m^3 mol^{-1} K^{-1}). The flux is then divided by soil surface area (m^2) and active denitrifying depth (0.1 m; Almaraz et al. 2020). To obtain a volumetric flux integrated over the pore volume, values are divided by soil porosity. The final N_2O flux is expressed as µmol m^{-3} h^{-1}.

For each plot, fifteen millilitres of pore water were sampled at three time points: before treatment, immediately after, and after the final gas measurement.

Automated field measurements in the Agali forest

A unique setup was implemented at the Estonian site of Agali, where an automated GHG monitoring system had been pre-installed, as described by Mander et al. (2021). This system used twelve automated chambers, spaced 5–15 m apart, to enable continuous N_2O monitoring with a PICARRO analyser. As at other sites, treatments were applied directly to the soil, and gas fluxes were monitored for one month following addition (June–July 2024). Treatments included (1) water only and 2) water + nitrate. Soil moisture and temperature were continuously recorded with pre-installed sensors (Campbell Scientific Inc. temperature probe; ML3 ThetaProbe soil moisture sensor), and pore-water sampling followed the same procedure as in other study sites.

Batch (slurry soil) incubations

Soil samples were collected from each site (three replicates per site) and stored at 4 °C in darkness to limit microbial activity before experimentation. For slurry soil incubations (hereafter referred to as batch incubations), approximately 20 mL of homogenised soil was placed in 150 mL glass bottles. Denitrifier Enzyme Activity (DEA), defined as the total production of $N_2O + N_2$, and the N_2O: ($N_2O + N_2$) ratio (RN_2O, which can be termed the efficiency of the hot moment), were determined using the acetylene inhibition technique (Tiedje et al. 1989). This method blocks N_2O reduction to N_2, allowing quantification of the total denitrification potential. Additionally, as batch incubations provided ideal environmental conditions for denitrification, the control condition without acetylene yielded the maximum potential N_2O hot moment of each tested soil.

To relieve nitrate limitation, all samples received 100 mg N L^{-1} KNO_3, resulting in two treatments: (1) nitrate only and (2) nitrate + acetylene (acetylene from PRODAIR, Aubervilliers, Seine-Saint-Denis, France). Because high N_2O yield and acetylene interference affect the LI-COR analyser, a G200 N_2O Analyser (Geotech, QED Environmental Systems Ltd., Coventry, UK) calibrated with a 100 ppm standard was used. Bottles were kept at 25 °C between sampling intervals.

Before incubation, all bottles were flushed with N_2 gas to ensure anoxia and promote full denitrification. N_2O concentrations were converted to µmol g^{-1} dry soil using Eq. (2).

$$N_2O \text{ net production} = N_2O \text{ partial pressure} \times \frac{PV}{RT} \times \frac{1}{DW} \quad (2)$$

Here, N_2O partial pressure is measured in ppm using the G200 analyser. DW refers to the dry weight of the soil sample (g), P is ambient pressure (Pa), T is recorded temperature (K), V is the gas volume in the bottle (m^3), and R is the ideal gas constant (Pa m^3 mol^{-1} K^{-1}). Net N_2O production is expressed as µmol g_{DW}^{-1}.

This value was subsequently converted to a volumetric flux (µmol m^{-3} h^{-1}) using bulk soil density (g cm^{-3}) for comparison with field and mesocosm results [see Eq. (3)]. Since batch experiments use homogenised soil, porosity was excluded from calculations.

$$N_2O \text{ volumetric flux} = N_2O \text{ net production} \times \text{bulk density} \times 10^6 \quad (3)$$

Aquacosm (mesocosm) experiments

Intact soil cores (10 cm depth × 10 cm diameter) were collected from each site and stored at 4 °C in darkness before experimentation. After returning from the field campaign, they were placed in the GHG-Aquacosme system (Kanaan et al. 2025), consisting of four aquariums, each containing three replicate cores from the same site. Hermetic caps sealed the core tops, and plastic tubing connected the system to a LI-COR gas analyser (LI-7820). Submersible pumps allowed for precise control of water level within the aquariums. Environmental variables such as air pressure and temperature were monitored continuously, and TOMST sensors within each core recorded temperature and soil moisture at 1-min intervals, and two Rhizon samplers were installed per core for pore-water collection.

The cores were placed on a 10 cm sand layer to reproduce natural capillarity. Demineralised water, enriched with 100 mg N L^{-1} KNO_3, was added to each aquarium until the water level reached just below the surface, creating near-saturation and anoxic conditions. These conditions, combined with nitrate enrichment, were intended to maximise denitrifier activity. N_2O fluxes were measured alternately using 5 min detection and 5 min air-flushing cycles. For each core, fifteen millilitres of pore water were sampled at the start, during, and at the end of each experiment (defined as the time point at which N_2O emissions ceased).

As in field experiments, gas accumulation rates were used to calculate N_2O fluxes (µmol m^{-3} h^{-1}) using Eq. 1. Denitrification efficiency (RN_2O) was computed as the total N_2O emitted divided by the total nitrate consumed over the same period. These values were then compared with RN_2O estimates from batch experiments.

Pore-water analyses

For each plot during field experiments, fifteen millilitres of pore water were sampled at three time points: before treatment, immediately after, and after the final gas measurement. For each core during aquacosm experiments, fifteen millilitres of pore water were sampled at the start, during, and at the end of each experiment. No water was sampled during batch incubations, as the initial chemical composition of each soil was already analysed in the other experiments, and the final composition was not considered critical as long as sufficient nitrate was added to create a maximal hot moment. All pore-water samples were kept at 4 °C in darkness until analysis for nitrate, organic acids, dissolved organic carbon (DOC), and dissolved nitrogen (DN) at the CRBE Platform for Physical and Chemical Analyses (PAPC, Univ. Toulouse UPS, INPT, CNRS, IRD). Nitrate and organic acids were quantified using a Thermo Fisher Dionex ICS-5000 + HPIC (Thermo Fisher Scientific, Sunnyvale, CA, USA), while DOC and DN were measured using a Shimadzu TOC-L analyser (Shimadzu Corporation, Kyoto, Japan). Initial DOC, DN, nitrate, and total organic acid concentrations are listed in Appendix Table 2.

Normalisation

Denitrification-driven N_2O hot moments are influenced by several environmental parameters, notably soil temperature, moisture, and nitrate concentration. Consequently, direct comparison of raw flux values may be confounded by these variables. To address this, normalisation was performed to adjust fluxes and to isolate the effects of experimental design. This was achieved using the adapted NEMIS framework for denitrification modelling, which conceptualises observed fluxes as the product of a potential maximum rate and limiting factors [Eq. (4)] (Hénault and Germon 2000; Peyrard et al. 2011; Martínez-Espinosa et al. 2022).

$$\mathrm{Denit}_{\mathrm{real}} = \mathrm{Denit}_{\mathrm{pot}} \times f_{\mathrm{Nitrate}} \times f_{\mathrm{Temp}} \times f_{\mathrm{Humid}} \quad (4)$$

In this formulation, the observed denitrification rate ($Denit_{real}$, in µmol m^{-3} h^{-1}, approximated by N_2O flux) is described as a function of the potential maximum rate of denitrification ($Denit_{pot}$, in µmol m^{-3} h^{-1}) and multiplicative, adimensional limitation factors for nitrate ($f_{Nitrate}$), soil temperature (f_{Temp}), and soil moisture (f_{Humid}). As the experiments tested the impact of nitrate addition, normalisation was not performed with $f_{Nitrate}$ in order to still be able to evaluate its effect. As for f_{Temp} and f_{Humid}, since soil temperature and moisture were systematically recorded during each experiment, normalised N_2O fluxes were computed by dividing the

measured fluxes by the product of the corresponding limitation factors [Eq. (5)].

$$\text{Normalised } N_2O \text{ flux} = \frac{\text{Raw } N_2O \text{ flux}}{f_{\text{Temp}} \times f_{\text{Humid}}} \quad (5)$$

This normalisation was applied to N_2O fluxes for field and aquacosm experiments. N_2O fluxes from batch incubations were not normalised, as they were supposed to already reach $f_{Temp} = 1$ (temperature controlled at 25 °C) and $f_{Humid} = 1$ (soil structure degraded and totally inundated). It facilitated comparison of flux data across methodologies and environmental conditions, improving the robustness of inter-experimental analyses. The formulations of the adimensional factors, ranging from 0 to 1, are given in Eq. (6–8).

$$f_{\text{Nitrate}} = \frac{\left[NO_3^-\right]}{K_{M,NO_3^-} + \left[NO_3^-\right]} \quad (6)$$

$[NO_3^-]$ is the initial soil nitrate concentration given in µmol N L^{-1}. $K_{M, NO3}$ is the apparent half-saturation constant of nitrate consumption, fixed at 17 µmol N L^{-1} according to Sihi et al. (2020).

$$f_{\text{Temp}} = \exp\left[-\frac{\left(\text{Temp}_i - \text{Temp}_{\text{opt}}\right)^2}{\text{Temp}_i \times \text{Temp}_{\text{opt}}}\right] \quad (7)$$

$Temp_i$ is the soil temperature in °C, and $Temp_{opt}$ is the optimal temperature for denitrification, fixed at 25 °C according to Sihi et al. (2020).

$$f_{\text{Humid}} = \frac{\text{Humid}_i - \text{Humid}_{\text{res}}}{\text{Humid}_{\text{sat}} - \text{Humid}_{\text{res}}} \quad (8)$$

$Humid_i$ is the soil moisture (m^3_{liquid} m^{-3}_{total}), $Humid_{res}$ is the minimal soil moisture possible (m^3_{liquid} m^{-3}_{total}; dependent on the type of soil), and $Humid_{sat}$ is the maximal soil moisture possible (m^3_{liquid} m^{-3}_{total}; dependent on the type of soil).

Statistical analyses

All statistical analyses were performed in Python using linear mixed-effects models (MixedLM, statsmodels), fitted by restricted maximum likelihood (REML) using the L-BFGS optimiser. Prior to analysis, N_2O fluxes were log-transformed to achieve normality and homoscedasticity. For datasets containing negative values, a constant (absolute minimum + 1.1) was added prior to transformation. Fixed effects included the factor of interest (normalisation, time of measurements, treatment, experiment) and its interaction with wetland type when relevant. Random effects accounted for repeated measurements within experimental units (site or unique plots), with random intercepts and, when appropriate, random slopes. Restoration actions were not consistent enough within a given wetland type to be statistically analysed, and thus are shown only for information purposes. Model formulas, hypotheses and effects are reported in Table S1. Post-hoc contrasts are presented in Table S2 and in Table S3 (for Fig. 5c). Descriptive statistics of Fig. 5 are presented in Table S4. Significance was assessed using Wald z-tests ($\alpha = 0.05$). In the Results and Discussion sections, LMM results for overall effects and descriptive statistics are expressed as mean ± standard deviation, whereas post-hoc contrasts between wetland types are expressed as mean ± standard error of the mean.

Results

Between May and July 2024, field campaigns were conducted in 21 European wetlands, including in situ experiments and soil sampling. For laboratory analyses, three intact soil cores and three slurry samples were collected from each site for mesocosm and DEA experiments, respectively. During field measurements, water or a water + nitrate solution was applied to induce a denitrification hot moment. In both mesocosm and DEA experiments, a water + nitrate treatment was likewise used to simulate such events.

Validation of experimental setups

To reduce differences attributable to soil moisture and temperature variations across study sites, and to compare N_2O fluxes between treatments, all raw fluxes were normalised to 25 °C and full water saturation, using Eq. (5). To assess the impact of this normalisation step, field N_2O fluxes measured 3 h after water or water + nitrate treatment were compared with their normalised equivalents (Fig. 2a). The initial soil moisture and temperature at each site are provided in Appendix Table 2. The effect of each treatment alone was assessed by comparing normalised

fluxes before and 3 h after treatment (Fig. 2b and c). Finally, to isolate the effect of nitrate addition, normalised N_2O fluxes were compared between water and water + nitrate treatment (Fig. 2d).

Across all sites, normalisation significantly increased N_2O fluxes (Fig. 2a; log-delta = 0.77 ± 0.08, $p < 0.001$). This effect was significant for all wetland types ($p < 0.03$) except for mountain peatlands ($p = 0.145$). The greatest effect, clearly visible on Fig. 2a, was observed for drained peatland forests, for which normalisation increased fluxes by more than five times (ratio = 5.06).

There was no overall statistically significant increase in N_2O fluxes after water treatment compared to the baseline (Fig. 2b; $p = 0.651$). When evaluating the effect within each wetland type, only open peatlands showed a significant modification, with fluxes after treatment less than half of the baseline (ratio = 0.45, log-delta = -0.7 ± 0.3, $p = 0.008$). For other wetland types, water addition did not significantly change the magnitude of fluxes. By contrast, water + nitrate treatment significantly increased overall N_2O fluxes compared to the baseline (Fig. 2c; log-delta = 1.60 ± 0.18, $p < 0.001$), and this effect was consistent among all wetland types ($p < 0.008$).

When testing for the effect of nitrate addition (i.e., comparing N_2O emissions 3 h after water or water + nitrate treatment), overall fluxes were significantly higher after water + nitrate treatment (Fig. 2d; log-delta = 0.7 ± 0.2, $p = 0.001$). However, this increase was only significant for mountain peatlands and open peatlands ($p < 0.005$), with fluxes respectively nearly 3 and 7 times higher. Alluvial forests and floodplains showed fluxes slightly higher after water + nitrate treatment, although the effect was not statistically significant ($p = 0.118$ and 0.406 respectively). Drained peatland forests also showed no significant difference between treatments (log-delta = 0.2 ± 0.3, $p = 0.560$). Across all sites, 78% of replicates showed higher N_2O fluxes following water + nitrate addition compared to water-only treatment.

Comparison across methods of N_2O hot moments dynamics

In this section, N_2O data from two sites (the Spanish alluvial forest of Tordera and the Estonian drained peatland forest of Agali) are presented to illustrate the complementary aspects provided by each method regarding the dynamics of denitrification-driven N_2O hot moments (Fig. 3).

In situ N_2O fluxes following water treatment remained close to zero in the Spanish alluvial forest, confirming that emissions in the water + nitrate treatment resulted from nitrate stimulation (Fig. 3a). Fluxes rose gradually between 1 and 3 h after treatment, followed by a decline between 16 and 19 h. Batch incubations (Fig. 3c) provided estimates of maximum N_2O fluxes at 3 and 6 h after nitrate addition, reaching 500 and 1,000 µmol m^{-3} h^{-1} for this alluvial forest. The difference between treatments with and without acetylene allowed estimation of total N_2 production during denitrification, approximately 2,000 µmol m^{-3} h^{-1} in this case. Continuous in situ measurements from the pre-installed system at the Agali site (see Materials and Methods) captured full emission dynamics over time (Fig. 3b). For the water treatment, one of the three replicates showed notable emissions up to 6,000 µmol m^{-3} h^{-1}, while the others showed no increase above the emission baseline. For the water + nitrate treatment, two replicates showed an increase in emissions, the highest reaching 6,000 µmol m^{-3} h. These data allowed estimation of both emission duration (ranging from 60 to 90 h) and peak magnitude (500–6,000 µmol m^{-3} h^{-1}).

Aquacosm fluxes from the Agali site are shown in Fig. 3d, enabling direct comparison between in situ and mesocosm dynamics. While aquacosm-derived N_2O fluxes were 2–50 times higher than those measured in the field, the bell-shaped emission curve and timing of the peak (30–70 h) were consistent across both methods.

N_2O emission rates across study sites

The N_2O flux measured 3 h after water + nitrate treatment was the only characteristic of N_2O hot moments consistently comparable across all three setups (Fig. 4).

No statistically significant difference was observed between the overall magnitude of N_2O fluxes in field and aquacosm experiments (Fig. 4a; $p = 0.084$). Among all wetland types, only open peatlands presented significantly higher fluxes in field experiments

(log-delta = 2.9 ± 1.0, p = 0.005), with a magnitude nearly 20 times higher than in aquacosm experiments.

In batch experiments, N_2O fluxes were consistently higher than those measured in aquacosms (Fig. 4b; log-delta = 2.3 ± 0.3, p < 0.001), ranging from 10^2 to more than 10^4 µmol m^{-3} h^{-1}. This trend was observed for all wetland types (p < 0.003), with the highest increase in floodplains (ratio = 28.42), open peatlands (ratio = 15.06), and mountain peatlands (ratio = 13.72).

Key determinants of N_2O hot moments

Aquacosm and batch experiments, as well as their comparison, helped quantify key determinants of N_2O emission dynamics, namely the duration and magnitude of emissions (from aquacosm experiment; Fig. 5a), N_2O: ($N_2O + N_2$) ratios (from aquacosm and batch experiments; Fig. 5b), and ratios of N_2O fluxes 3 h after treatment between aquacosm and batch experiments (Fig. 5c).

The duration of N_2O emissions in aquacosm experiments varied substantially among sites (Fig. 5a; mean = 50 ± 40 h). Floodplains consistently completed emissions within less than 24 h (mean = 14 ± 5 h), whereas other wetlands ranged from 10 to over 150 h. Half of the drained peatland forest replicates did not show a decline in emissions; instead, they remained stable or increased, necessitating experiment termination before N_2O emissions ceased. These forests also displayed the highest maximum N_2O fluxes, reaching up to 25,000 µmol m^{-3} h^{-1}. Floodplains, open and mountain peatlands, and alluvial forests had flux peaks from 30 to 12,000 µmol m^{-3} h^{-1}, with alluvial forests presenting the greatest variability (mean = 3,000 ± 3,000 µmol m^{-3} h^{-1}). A significant positive correlation was observed between overall duration and maximal magnitude of N_2O fluxes (p < 0.001).

Figure 5b shows RN_2O values calculated from aquacosm and batch experiments (see Materials and Methods). Nearly half of aquacosm values remained between 0 and 0.1 (46% of replicates; mean of all values = 0.09 ± 0.40), except in drained peatland forests where they reached up to 1.5. Additionally, 34% of replicates showed RN_2O values below 0, and 5% above 1. Batch RN_2O values exhibited greater variability and inconsistencies (mean = 2 ± 10), with 32% of replicates exceeding 1 and none below 0. Due to this high variability, no significant difference was detected between aquacosm and batch RN_2O values (p = 0.177). When focusing on values between 0 and 1 (theoretical range, as $RN_2O = N_2O$: ($N_2O + N_2$)), batch values were significantly higher than aquacosm values (delta = 0.41 ± 0.08, p < 0.001).

Figure 5c highlights the differences between aquacosm and batch N_2O fluxes. Except for one replicate with a negative flux ratio (due to a negative value of N_2O flux in aquacosm experiments), all ratios were between 0 and 0.95, signifying that aquacosm-derived fluxes were systematically lower than batch fluxes. Ratios for alluvial forests displayed the widest variability (mean = 0.3 ± 0.3), while ratios for floodplains and open peatlands did not exceed 0.15 (respectively, mean = 0.03 ± 0.05 and 0.03 ± 0.04), consistent with their extremely low aquacosm N_2O fluxes (Fig. 5a). All other wetland types showed ratios below 0.3. Pairwise comparisons among wetland types revealed a single significant difference: alluvial forests differed from open peatlands (Holm-adjusted p = 0.042), while no other contrasts were statistically significant.

Discussion

Each experimental approach successfully provoked high transient N_2O emissions, and their comparison helped characterise different aspects of these hot moment dynamics. Substantial variability was observed throughout the measurements, possibly attributable to initial environmental conditions or alternative N_2O-producing pathways.

Reproducing denitrification-driven N_2O hot moments

Baseline emissions were frequently substantial: 24% of replicates exceeded 10 µmol m^{-3} h^{-1} and some drained peatland forests surpassed 100 µmol m^{-3} h^{-1} (Fig. 2b and c). Most replicates (65%) ranged between 0 and 10 µmol m^{-3} h^{-1}. These values confirm that natural wetlands can act as persistent N_2O sources (Pärn et al. 2018; Mander et al. 2021; Christensen & Rousk 2024), with emissions amplified after an environmental perturbation affecting nitrate availability. A minority of measurements (11% of replicates) showed negative baseline fluxes, indicating net N_2O uptake.

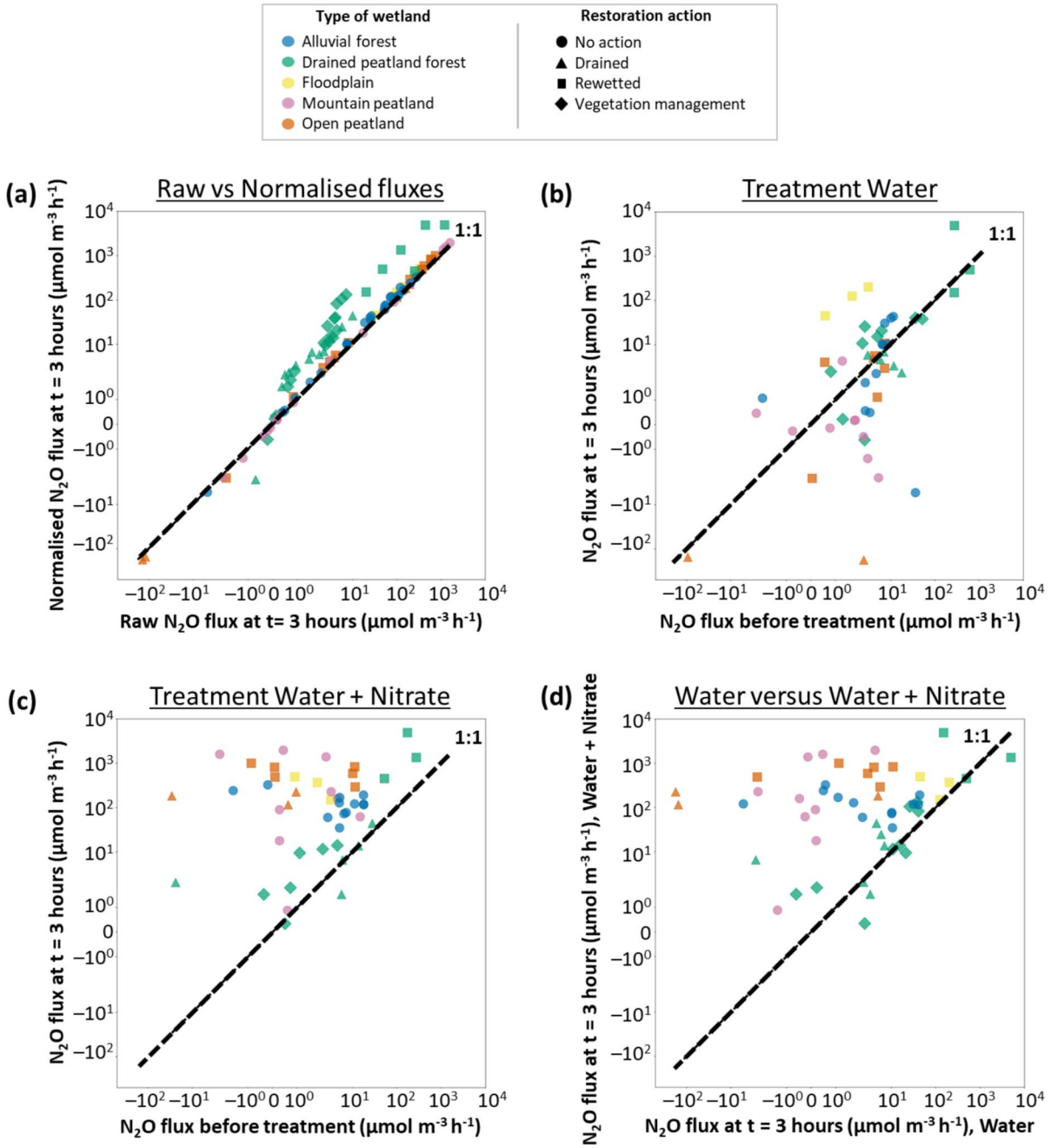

Fig. 2 Comparison of field N_2O fluxes for all study sites, symmetric-log scale. To ensure linearity on the symmetric-log scale, the axis scales are smaller between -10^0 and 10^0. **a** Fluxes measured 3 h after water or water + nitrate treatment, raw versus normalised. **b** Normalised fluxes measured before and 3 h after water treatment. **c** Normalised fluxes measured before and 3 h after water + nitrate treatment. **d** Normalised fluxes measured 3 h after treatment, water versus water + nitrate

These values were never observed consistently within a single site and were not correlated with measured initial physico-chemical properties (listed in Appendix Table 2). They may reflect localised lower soil

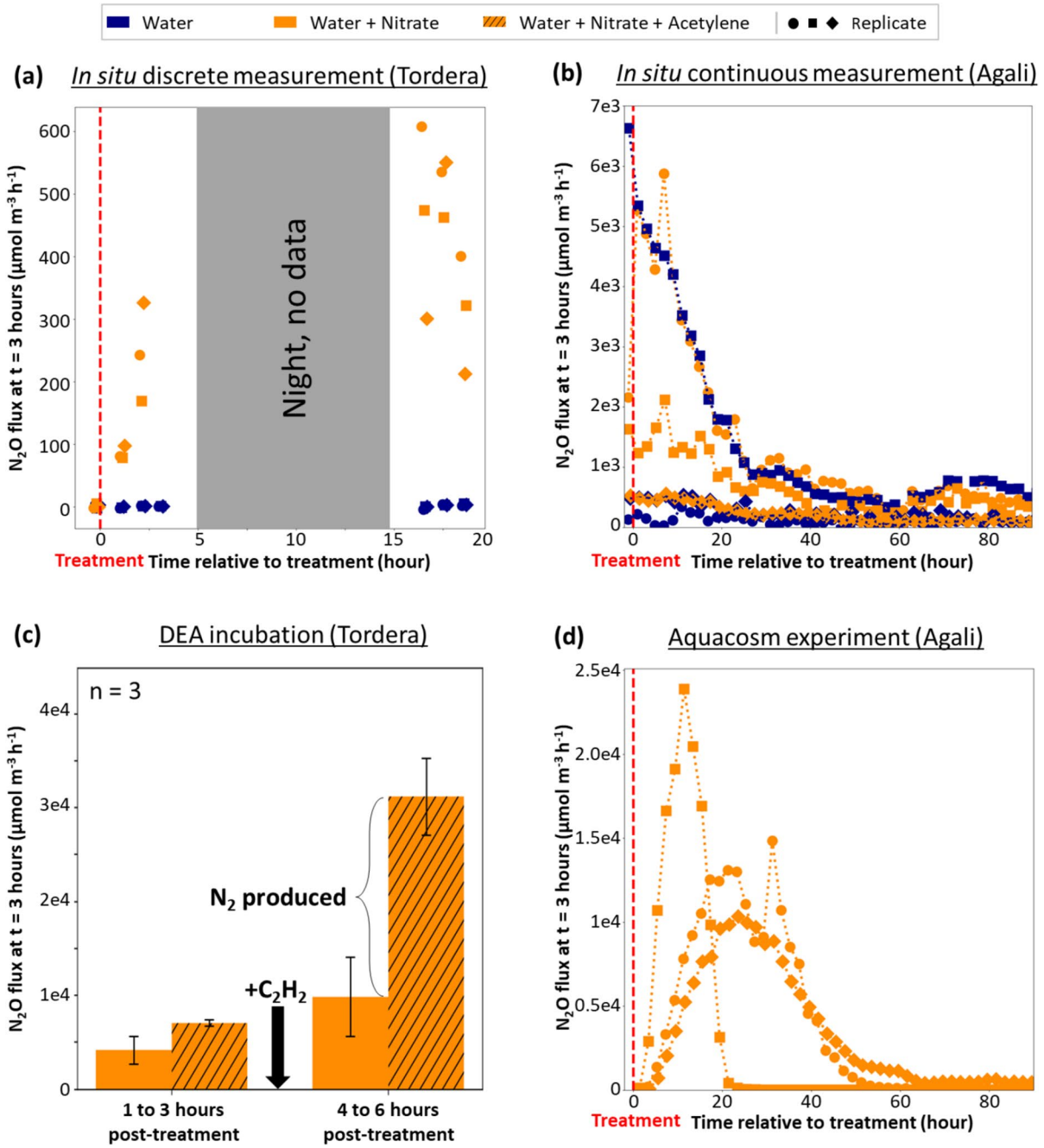

Fig. 3 Examples of normalised N_2O fluxes observed during each experiment. **a** In situ measurements, Spanish site of Tordera. **b** Continuous in situ measurement, Estonian site of Agali. **c** Batch incubations with and without acetylene, Spanish site of Tordera; acetylene added between 3 and 4 h after incubation start. Error bars denote the standard error of the mean. **d** Aquacosm experiments with intact cores, Estonian site of Agali

moisture not captured by the probe, as dry soils have occasionally been reported to act as N_2O sinks (Goldberg & Gebauer 2009).

In field experiments, water addition alone did not significantly alter N_2O fluxes relative to baseline (Fig. 2b; $p = 0.651$), except in open peatlands

where fluxes were reduced by half (ratio = 0.45, log-delta = − 0.7 ± 0.3, p = 0.008). Water + nitrate addition, by contrast, significantly increased fluxes (Fig. 2c; log-delta = 1.60 ± 0.18, p < 0.001), with a consistent effect among all wetland types. At the Agali site, the only location equipped for continuous field monitoring (Fig. 3b), emissions persisted for 2–4 days following nitrate addition. As these in situ N_2O emissions were induced by an environmental perturbation (water + nitrate addition), reached high values compared to the baseline (Fig. 2c; log-delta = 1.60 ± 0.18), and lasted only for a short time (Fig. 3b; 60–90 h), they meet the definition of N_2O hot moments (Groffman 2012).

A direct comparison between the water-only and water + nitrate treatments further highlights the effect of nitrate alone, with higher N_2O emissions observed under the water + nitrate treatment (Fig. 2d; log-delta = 0.7 ± 0.2, p = 0.001), indicating that nitrate stimulated these hot moments. Because denitrification consumes nitrate to produce N_2O, this nitrate dependence is consistent with a denitrification-driven mechanism. These soils may have contained the conditions required to trigger a hot moment but were likely limited by nitrate availability, supporting the interpretation of these events as denitrification-driven N_2O hot moments. When focusing on wetland types, this response was significant only in mountain peatlands and open peatlands, whereas alluvial forests also showed higher fluxes after water + nitrate treatment, although not statistically significant (log-delta = 0.5 ± 0.3, p = 0.118). According to Appendix Table 2, these sites had initial nitrate concentrations below 1.5 mg N L^{-1}, supporting this interpretation of nitrate limitation. Only one floodplain was measured in situ, preventing any robust conclusion from being drawn. Drained peatland forests showed no response to water + nitrate compared to water-only (log-delta = 0.2 ± 0.3, p = 0.560), suggesting low nitrate constraints on these emissions. Two drained peatland forests exhibited initial nitrate concentrations of 3.5 and 20.9 mg N L^{-1}, supporting the hypothesis of

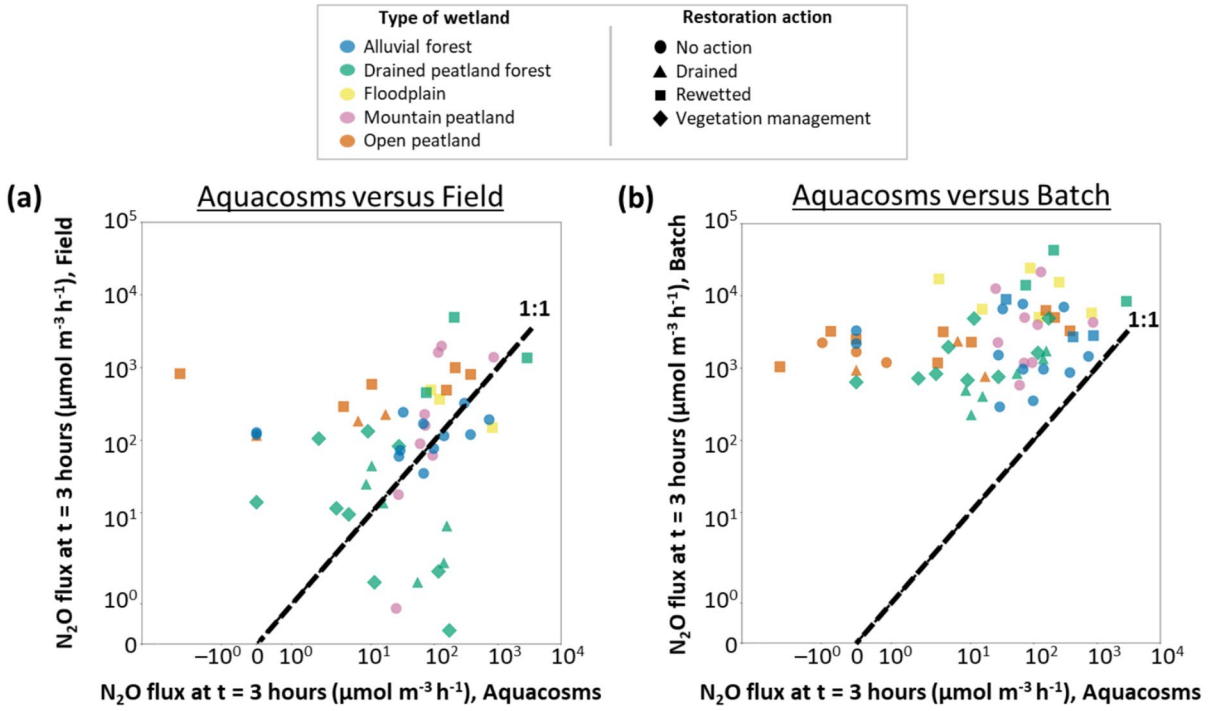

Fig. 4 Normalised N_2O fluxes for all study sites, measured 3 h after water + nitrate treatment, symmetric-log scale. To ensure linearity on the symmetric-log scale, the axis scales are smaller between -10^0 and 10^0. **a** Field versus aquacosm fluxes. **b** Batch versus aquacosm fluxes. More data points appear in **b** because in situ measurements were not feasible at all sites owing to technical constraints

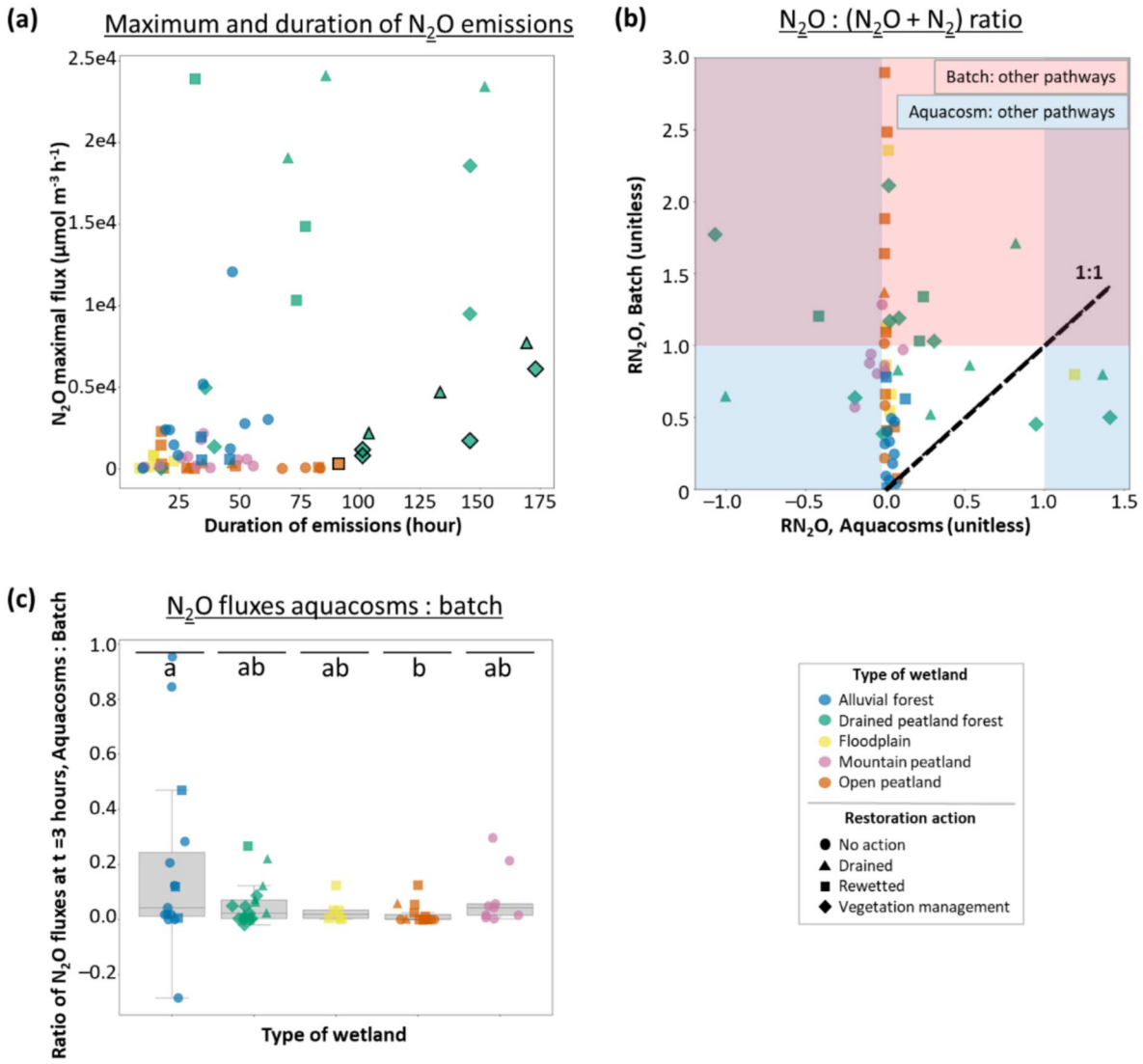

Fig. 5 Key determinants of N_2O hot moments after water + nitrate treatment. **a** Duration of emission and maximal flux in aquacosms; replicates are outlined when emissions remained stable or increased. **b** Comparison of RN_2O between aquacosm and batch experiments; the red zone highlights batch RN_2O values exceeding 1, blue zones show aquacosm RN_2O values below 0 or above 1. **c** Ratio of N_2O fluxes (aquacosm: batch) measured 3 h after treatment; letters indicate significant differences among wetland types based on linear mixed-effects models (site as a random factor) with Holm-adjusted pairwise comparisons ($p < 0.05$)

an excess of nitrate in these sites, although the same trend appeared in other drained peatland forests with lower nitrate contents. Field experiments therefore provide an ecologically realistic framework to reproduce denitrification-driven N_2O hot moments and capture their expression under intact soil conditions (O'Connell et al. 2022).

At the Agali site, where continuous in situ measurements enabled direct comparison with mesocosm experiments, aquacosm reproduced both the shape and timing of field emissions, though with flux magnitudes 2 to 50 times higher (Fig. 3b, d). The bell-shaped emission curve of these N_2O peaks is typical of denitrification hot moments following nitrate

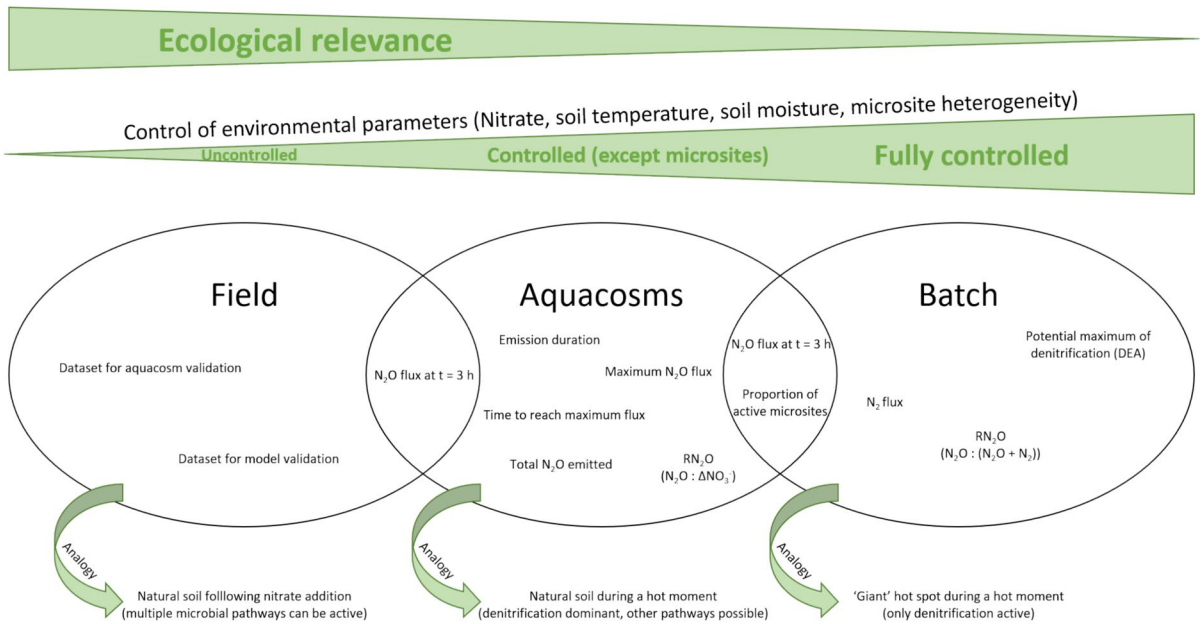

Fig. 6 Summary of the strengths, limitations, and applications of field, aquacosm, and batch experiments for studying denitrification hot moments

addition (Frostegård et al. 2022). When comparing aquacosm and field results across all sites, flux magnitudes were largely similar (Fig. 4a; $p = 0.084$), suggesting that aquacosms can be considered reliable proxies for simulating denitrification-driven N_2O hot moments in structured soils (Kanaan et al. 2025).

N_2O fluxes measured 3 h after water + nitrate treatment were 4 to 30 times higher in batch incubations than in aquacosm and field measurements (Fig. 4b; ratio = 4.64 in alluvial forests and 28.42 in floodplains). This indicates that slurry soil incubations created near-optimal conditions for denitrification-driven N_2O hot moments, producing fluxes that were maximised yet less ecologically realistic. Free from structural constraints and environmental heterogeneity, batch incubations can therefore be interpreted as approximations of large-scale denitrification hotspots, where N_2O emissions approach their theoretical maximum (Friedl et al. 2020).

Characterising the dynamics of hot moments

Single-point field measurements alone were insufficient to capture the full dynamics of N_2O hot moments. Although nitrate addition was followed by hour-scale N_2O emissions (Fig. 3a), discrete field measurements could not resolve key dynamic features such as peak intensity or emission duration. These were successfully quantified in aquacosm experiments (Fig. 5a), where N_2O emissions ranged from 10 to 150 h and maximal fluxes reached 25,000 µmol m^{-3} h^{-1}, illustrating the short-lived yet highly intense N_2O fluxes characteristic of denitrification hot moments. Among wetland types, drained peatland forests exhibited the highest and most variable fluxes (mean = 10,000 ± 9,000 µmol m^{-3} h^{-1}) and the longest duration (mean = 100 ± 50 h). The second highest fluxes were observed in alluvial forests (mean = 3,000 ± 3,000 µmol m^{-3} h^{-1}), whereas all others wetland types presented fluxes below 2,500 µmol m^{-3} h^{-1}. These contrasting results confirm that the identification of N_2O hot moments must be contextualised according to ecosystem type. The observed ranges of N_2O emission magnitude and duration across wetland types (listed in Table S4) provide ecosystem-specific reference ranges that illustrate the typical characteristics of nitrate-induced hot moments. These values are intended to provide contextual reference points rather than universal thresholds. The variable timing, expanding up to six days, explains why capturing complete hot moments in situ

was challenging, as night-time measurements were impracticable.

One of the main difficulties in understanding and predicting denitrification hot moments is that these high and transient emissions only occur within microbially active microsites that meet the physico-chemical conditions necessary for denitrification (Chen et al. 2018; Schlüter et al. 2025). The main distinction between aquacosm and batch experiments was that intact cores retained soil structure and were therefore subject to diffusion limitations and heterogeneity in active microsites. These constraints could have led to localised oxic conditions or spatial heterogeneity in carbon and nitrogen distribution, potentially shifting microbial activity toward N_2O-producing pathways alternative to denitrification. Batch experiments, conducted using slurry samples with homogenised environmental conditions, likely experienced significantly reduced diffusion limitations and therefore provided optimised conditions for denitrification, maximising the proportion of active denitrifying microsites. A comparison between slurry and core experiments could thus inform on differences in N_2O production attributable to soil structure and heterogeneity, providing an estimate of the proportion of active microsites. Figure 5c illustrates this comparison by dividing volumetric N_2O fluxes in batch incubations by those in aquacosms.

Because batch experiments are assumed to produce N_2O primarily through denitrification, whereas aquacosms may also retain alternative N_2O-producing pathways, this ratio likely overestimates the true proportion of denitrifying microsites. Nevertheless, the aquacosm: batch N_2O flux ratio provides a first approximation of the influence of soil structure on denitrification-driven N_2O hot moments by relating maximal potential denitrification activity to ecologically realistic fluxes. Apart from one negative outlier, ratios ranged between 0 and 0.95, supporting the coherence of this approximation, with 95% of replicates below 0.3. Alluvial forests displayed the greatest variability, unrelated to carbon or nitrogen content (Appendix Table 2). We encourage future studies to refine this approach by minimising the contribution of alternative N_2O-producing pathways in structured soils, for example by combining flux measurements with isotopic analyses, selective inhibitors, or molecular approaches targeting denitrification genes (Wrage et al. 2004; Wallenstein and Vilgalys 2005; Hu et al. 2015). Once improved, this ratio may offer a simple yet informative metric to quantify microscale heterogeneity in denitrification, a long-standing challenge for both experimental and modelling studies (Wang et al. 2019; Schlüter et al. 2025).

Detection of possible alternative N_2O-producing pathways

The normalisation of N_2O fluxes was intended to correct for the impact of soil heterogeneity on denitrification, particularly differences in soil temperature and moisture. Because field and aquacosm experiments both preserved soil structure and diffusion effects, normalised N_2O fluxes were expected to be similar between the two approaches. This pattern was observed when considering all replicates together (Fig. 4a; $p = 0.084$); however, among wetland types, only open peatlands showed significantly higher fluxes in field conditions compared to aquacosm experiments (log-delta $= 2.9 \pm 1.0$, $p = 0.005$). For these sites, this difference may reflect the contribution of additional N_2O-producing pathways in field experiments, resulting in higher fluxes. Because aquacosm experiments provided fully saturated conditions, whereas in situ experiments involved only partial water saturation, it can be hypothesised that a substantial proportion of oxic microsites was present in the field, providing favourable conditions for oxic metabolisms such as nitrification. This interpretation is consistent with previous findings at the Agali site (Appendix Table 1), where drained soils exhibited higher N_2O emissions attributed to nitrification, while rewetted soils showed lower emissions mainly associated with denitrification (Masta et al. 2024).

In aquacosm experiments, the RN_2O ratio was calculated by dividing the total N_2O emitted by the difference in soil nitrate concentration between the beginning and the end of emissions (see Materials and Methods). Assuming denitrification was the only process capable of consuming nitrate and producing N_2O in these soils, RN_2O would represent denitrification efficiency and theoretically range between 0 and 1. It was inferior or equal to 0.1 for 46% of replicates (Fig. 5b), consistent with values used in existing denitrification models (e.g. 0.1 in Guilhen et al. 2020; 0.02 in Scheer et al. 2020). However, 34% of

replicates showed values below 0, indicating a negative denominator and thus nitrate net production during the experiment. This production may be attributable to nitrification, which can produce N_2O as a by-product. Similarly, 5% of replicates showed values exceeding 1, indicating N_2O production greater than nitrate consumption, which would be impossible if denitrification were the sole N_2O-producing pathway. Such anomalous values occurred mostly in drained peatland forests, consistent with Masta et al. (2022), who identified a minor but non-negligible contribution of DNRA and nitrification to N_2O production in drained wetlands after rewetting. However, the extent of these pathways remains uncertain, and even RN_2O values between 0 and 1 cannot be assumed to reflect denitrification alone. Future DNA- or RNA-based analyses targeting nitrification, denitrification, and DNRA, or isotope tracing of added nitrogen, would better resolve the contribution of each pathway and improve interpretation of these results (Wrage et al. 2004; Wallenstein and Vilgalys 2005).

By contrast, batch experiments provided near-ideal conditions for denitrification: saturated, homogenised soils with nitrate enrichment and constant temperature. The high N_2O fluxes observed (Fig. 4b) are therefore most plausibly attributed to denitrification. Moreover, as emphasised by Hu et al. (2015), in situ fluxes are commonly orders of magnitude lower than those measured under fully controlled laboratory conditions due to strong spatio-temporal variability and environmental constraints in the field.

High variability in N_2O emissions

Open peatlands showed low emissions in field and aquacosm trials (Figs. 4a and 5a). As these soils were already saturated (0.60–0.72 initial soil moisture; Appendix Table 2), added water likely failed to transport nitrate effectively, limiting denitrification.

Alluvial forests exhibited the highest variability in the aquacosm: batch N_2O flux ratio (Fig. 5c; mean $= 3{,}000 \pm 3{,}000$ µmol m^{-3} h^{-1}). The highest ratios, above 0.3, were recorded in sites with low initial soil moisture (0.35–0.48; Appendix Table 2). These sites (Confluent dry, Rhinau, and Canoves) experience quasi-permanent dry conditions (Appendix Table 1), and rewetting likely disturbed denitrifier communities, increasing the proportion of active N_2O-producing microsites. This pattern agrees with Vidon et al. (2016) and Richardson et al. (2025), who reported short, intense N_2O bursts after rewetting long-term dry soils.

Drained peatland forests showed the highest variability across all setups (Fig. 4a, b), with both the greatest emission magnitude and longest duration (Fig. 5a; duration $= 100 \pm 50$ h, maximum $= 10{,}000 \pm 9{,}000$ µmol m^{-3} h^{-1}). Like alluvial forests, half of these sites had low initial soil moisture (below 0.5) and long-term dry conditions (Appendix Tables A1 and A2), possibly explaining their variability and high emissions, as observed by Ranniku et al. (2024) at Agali. Figure 2a highlights their particular case, as these were the sites for which correction by soil moisture and temperature strongly modified N_2O fluxes (ratio = 5.06). Because their initial temperature did not differ markedly from other wetland types, it can be hypothesised that the main correction effect was related to low soil moisture, even after treatment addition. Additionally, as drained peatland forests were associated with the possible presence of other N_2O-producing microorganisms, these alternative pathways may also have contributed to their elevated emissions.

More broadly, replicate variability (illustrated at Agali; Fig. 3b, d), highlights the strong spatial heterogeneity and limited predictability of N_2O emissions in wetland soils. Unexpectedly high N_2O emissions following water treatment (one replicate in Fig. 3b) further underscore the complexity of denitrification-driven N_2O hot moments. In this particular case, the soil may already have contained high nitrate concentrations, as suggested by the high and variable initial nitrate levels at the Agali site (Appendix Table 2), and thus water addition alone may have triggered a localised denitrification hotspot. Understanding denitrification at fine spatial scales is necessary to identify consistent responses to nitrate addition and to improve quantification of global terrestrial N_2O emissions. The proportion of actively denitrifying soil volume estimated here may contribute to resolving these heterogeneous hotspots.

Limitations in result interpretation

Because normalisation did not alter the general trends of N_2O fluxes but mainly affected their magnitude (Fig. 2a), it appears to offer a reasonable correction for soil temperature and moisture variability, isolating

the effect of nitrate addition. Nevertheless, its formulation could be improved. Specifically, using a fixed optimal temperature (25 °C) may not reflect microbial optima across all regions. For instance, denitrifiers in northern Finnish soils may be adapted to cooler temperatures than those in southern Spain. As emphasised by Powlson et al. (1988), no universal temperature optimum exists for denitrification, and the standard value of 25 °C used in many models likely oversimplifies complex microbial responses. Future models should therefore adopt site-specific temperature optima to improve predictive accuracy.

In addition, normalisation accounted only for environmental parameters measured at the time of flux monitoring, such as initial and instantaneous soil temperature and moisture. However, microbial activity may depend on antecedent conditions. Seasonal cycles, short droughts, or prior rewetting (Hernandez & Mitsch 2006) could have legacy effects on denitrification potential. Incorporating such temporal dynamics into models will be essential for more reliable predictions of N_2O emissions.

Batch-derived RN_2O values represent the classical approach to estimate denitrification efficiency. They provide a point estimate of N_2O relative to $N_2O + N_2$ fluxes, determined by inhibiting the final step of denitrification (see Materials and Methods). These values showed substantial variability and often exceeded 1 (in 32% of replicates; Fig. 5b), suggesting that acetylene may have influenced net N_2O production beyond simple inhibition of N_2O reduction. This supports recurring criticism of DEA assays, which highlight acetylene interference with microbial activity, as acetylene can inhibit N-cycle metabolisms such as nitrification and denitrification (Tilsner et al. 2003; Felber et al. 2012). Moreover, DEA assays have been shown to be less efficient in wet soils due to the limited acetylene diffusion in water (Tilsner et al. 2003). When restricting values to the theoretical range of [0, 1], batch RN_2O values remained significantly higher than aquacosm values (Fig. 5b), suggesting possible overestimation linked by acetylene interference.

Thus, both aquacosm- and batch-derived RN_2O ratios present limitations. Batch experiments maximise denitrification and ensure it remains the dominant process; however, RN_2O determination is restricted to the first hours following water + nitrate addition and may not represent realistic ratios in natural soils. Furthermore, acetylene inhibition itself may lead to overestimation of the ratio. Aquacosm RN_2O values integrate emissions over the entire experimental period and directly relate N_2O production to nitrate consumption, making them potentially more representative of field conditions. However, because soil structure is preserved, aquacosms may also sustain alternative N_2O-producing and nitrate-consuming pathways that could bias ratio estimation. Despite these limitations, aquacosm-derived RN_2O values should be preferred over batch-derived values for characterising and simulating denitrification-driven N_2O hot moments, as they better reflect structured soil conditions. N_2O fluxes from batch incubations presented in Figs. 4b and 5c, as they were measured without acetylene, were free from these perturbations. By inducing the maximal potential hot moment for each soil, this experiment provided the upper range of N_2O fluxes attributable to denitrification, enabling comparison with structured soils.

The estimation of active soil volume (Fig. 5c) also merits discussion. N_2O fluxes 3 h post-treatment under diffusion-limited versus diffusion-free conditions may not be directly comparable, as the rate of N_2O consumption (last step of denitrification) might differ between setups, leading to inaccurate comparison of two different dynamics. In addition, denitrification may not have been the sole pathway producing N_2O in these experiments (especially in field and aquacosm experiments), where alternative processes could bias estimates of the proportion of actively denitrifying soil. Nevertheless, this ratio-based approach has the advantage of being simple to apply across multiple sites and provides a first approximation that can guide the development of refined methods. Analysis of nitrogen stable isotope abundance throughout the soil profile could further clarify the influence of diffusion and microsite heterogeneity on N_2O production (Goldberg et al. 2008). Several studies have applied this approach to assess the effects of drought (Goldberg & Gebauer 2009; Berger et al. 2013b in East Asian forest soils), drying/rewetting cycles (Goldberg et al. 2010; Berger et al. 2013a in South Korean rice paddies), and freeze/thaw events on N_2O production and consumption in diverse soils. Using this method, these authors were able to determine more precisely the depth and magnitude of N_2O emissions following such perturbations.

Importance for modelling efforts

Most denitrification models estimate daily or annual mean N_2O fluxes, typically through simplified geophysical formulations (Heinen 2006; Martínez-Espinosa et al. 2022). The short-lived N_2O hot moments observed in this study (10–150 h in aquacosm experiments; Fig. 4a) emphasises the need for hourly-resolution models to accurately simulate and predict these emissions. The challenge of incorporating small-scale heterogeneity in global models has been well documented (Or 2020; Del Grosso et al. 2020), and the solution relies on a balance between detailed, metabolism-based formulations, and data availability and resolution. Microbial and enzymatic controls are particularly important during transient hot moments, when microbial kinetics, rather than bulk environmental drivers, govern emissions. As slurry soil experiments allow controlled perturbations (e.g., acetylene addition) under stable conditions, they are well-suited for studying these aspects. Future studies on microbial-based models are encouraged to focus on these types of experiments to calibrate enzymatic parameters and transient dynamics.

Wang et al. (2019) proposed to consider the soil as a matrix containing a defined volume of active micro-aggregates to comprehend and quantify GHG exchanges from soil. This conceptualisation, associated with a microbial-based formulation of denitrification (Ebrahimi & Or 2016), might be key to predict and reproduce N_2O hot moments in heterogeneous hotspots. The estimated fraction of actively denitrifying soil (Fig. 5c) provides an attempt to quantify these micro-aggregates. Future models should incorporate this spatial heterogeneity to accurately simulate N_2O hotspots and hot moments.

Most denitrification models employ a single RN_2O value (Guilhen et al. 2020; Scheer et al. 2020). We argue that the experimental calibration of this ratio should be subject to extreme caution, as it strongly depends on methodology and may be influenced by other N_2O-producing pathways. Notably, batch-derived RN_2O estimations may be affected by acetylene, whereas aquacosm-derived values may include non-denitrification processes, leading to incorrect estimations (Fig. 5b). As Weier et al. (1993) noted, using a universal RN_2O for diverse ecosystems may lead to false estimations as N_2O-producing soils can be considerably different from each other, and global models should apply wetland-type-specific or condition-specific values.

Finally, the wide geographical and ecological scope of this study (covering diverse wetland types, climates, and latitudes) produced a unique dataset of N_2O emissions following nitrate addition. Combined with high-resolution aquacosm data and fully controlled batch data, field observations provide a solid empirical foundation for calibrating and validating models that simulate denitrification N_2O hot moments in wetlands. We strongly encourage using multiple ecosystems and complementary experimental methods to ensure the scalability and robustness of future models.

Conclusion

By integrating three complementary approaches (in situ measurements, intact core experiments, and slurry soil incubations) across a broad range of European wetlands, this study established a framework for characterising denitrification-driven N_2O hot moments. Aquacosms, which reproduced the shape and timing of field N_2O emission peaks, captured the complete dynamics of these transient events, including peak magnitude, emission duration, and RN_2O values. The combination of aquacosm and batch incubations, in turn, could provide a novel way to estimate indirectly the proportion of soil microsites actively contributing to N_2O emissions. These findings warrant further validation through external techniques such as tomography or microprobe analyses, and should be the focus of future investigations. A synthesis of each method's contributions and limitations is presented in Fig. 6.

The key determinants derived from this integrated approach (RN_2O, flux intensity, emission duration, and proportion of active microsites) span a wide range of wetland types, latitudes, and environmental contexts. We encourage the use of these parameters to calibrate future microbial-based denitrification models aiming to simulate N_2O emissions during denitrification hot moments. Field measurements remain essential for model validation, anchoring laboratory

and mesocosm results in real ecological conditions. By providing a robust experimental dataset for the calibration and validation of predictive models, this study supports a more accurate and scalable understanding of wetland N_2O emissions, essential for guiding mitigation strategies and ecosystem management under global change scenarios.

Acknowledgements The authors thank Tuija Hytönen for preparing treatment solutions for Estonia and Finland, and Mauri Heikkinen and Juuli Suominen for their skilled technical assistance during Finnish field campaigns. We thank Richard Peter from the Conservatoire d'Espaces Naturels (CEN; Center of Natural Reserves) of Alsace for providing access to the Eastern French site of Rhinau. We also thank the Observatoire Homme-Milieux Pyrénées (OHM; Man-Ecosystem Observatory) of Haut-Vicdessos, LABEX DRIIHM (ANR-11-LBX-0010), and the Service National d'Observation Tourbières (SNO; French Peatland Observatory), part of the OZCAR research infrastructure, for granting access to the Bernadouze site in the French Pyrenees. We are deeply grateful to Frédéric Julien, Didier Lambrigot, Corinne Pautot and Virginie Payre-Suc of the CRBE Platform for Physical and Chemical Analyses (PAPC, Univ. Toulouse UPS, INPT, CNRS, IRD) for conducting all pore-water analyses. We also acknowledge the financial support from the French Ministère de l'Enseignement supérieur, de la Recherche et de l'Innovation (MESRI; French Ministry of Higher Education, Research and Innovation) through the 'allocation doctorale' grant.

Author contributions Thomas Crestey-Chury, Romain Darnajoux, Sabine Sauvage, Thierry Camboulive, Noémie Carles, José-Miguel Sánchez-Pérez designed and conducted the field experiments across all study sites and performed the corresponding laboratory analyses in the CRBE laboratory. Thomas Crestey-Chury carried out data curation, analysis, and visualisation, with contributions from Romain Darnajoux, Sabine Sauvage, and José-Miguel Sánchez-Pérez, and wrote the manuscript with input from all co-authors. José-Miguel Sánchez-Pérez supervised the study. Tuula Larmola provided LI-COR gas analysers, contributed to the acquisition of flux and environmental data for in situ measurements, and participated in soil samplings in southern Finland. Local sites supervisors included Jyrki Jauhiainen (northern Finnish sites), Laure Gandois (French site of Bernadouze), Tuula Larmola, Liisa Ukonmaanaho, Mika Aurela and Sari Juutinen (southern Finnish sites), Ülo Mander, Kaido Soosaar (Estonian sites), Maud Raman (Belgian sites), Francesc Sabater (Spanish sites), and José-Miguel Sánchez-Pérez (other French sites). Additional on-site support was provided by Tom De Dobbelaer (Belgium), Laura Escarmena and Sílvia Poblador (Spain), and Thomas Schindler and Kaido Soosaar (Estonia).

Funding This research has been conducted with the support of the ALFAwetlands, wetland restoration for the future project Horizon Europe n°101056844, an EU-funded initiative under the Horizon Europe program, aimed at enhancing European wetland management for greenhouse gas mitigation and biodiversity conservation.

Data availability The experimental datasets generated and analysed during the current study are available from the corresponding author, Thomas Crestey-Chury, upon reasonable request.

Declarations

Competing interests The authors have no relevant financial or non-financial interests to disclose.

Appendix

See Tables 1 and 2.

Table 1 Summary of all study sites with their wetland type, state of restoration, and detailed description

Country	Site name	Type of wetland	Restoration action (water regime change)	Description
Belgium	Dyle Valley	Floodplain	Rewetted	Alluvial floodplain with buried peat; grazing area
Belgium	Zuidleie Valley	Open peatland	Rewetted	Mesotrophic fen meadow; manual removal of sludge deposit
Belgium	Zwarte Beek	Floodplain	Rewetted	Floodplain with buried peat; rewetted by closing ditches
Estonia	Agali	Drained peatland forest	Rewetted	Rewetted naturally (beaver)
Estonia	Kuresoo	Open peatland	Rewetted	Rewetted former drained peatland
Estonia	Kuresoo Control	Open peatland	No action	Peatland
Estonia	Laiuse	Open peatland	Rewetted	Rewetted former peat extraction field; water level manipulation
Estonia	Laiuse Control	Open peatland	Drained	Former peat extraction field
Finland	Kivalo	Drained peatland forest	Vegetation management	Continuous cover forestry on drained peatland forest
Finland	Kivalo Control	Drained peatland forest	Drained	Drained peatland forest
Finland	Lettosuo	Drained peatland forest	Vegetation management	Continuous cover forestry on drained peatland forest
Finland	Lettosuo Control	Drained peatland forest	Drained	Drained peatland forest
Finland	Rottasniitunsuo	Drained peatland forest	Vegetation management	In restoration: removal of trees
France	Bernadouze	Mountain peatland	No action	Non-productive mountain peatland
France	Confluent dry	Alluvial forest	No action	Rarely flooded
France	Confluent wet	Alluvial forest	No action	Flooding area
France	Rhinau	Alluvial forest	No action	Rarely flooded
Spain	Cànoves	Alluvial forest	Rewetted	Receiving effluents from a wastewater treatment plant
Spain	Estanyeres	Mountain peatland	No action	Non-productive mountain peatland; grazing area
Spain	Rubió	Mountain peatland	No action	Non-productive mountain peatland; grazing area
Spain	Tordera	Alluvial forest	No action	Flooding area

Table 2 Soil initial conditions. Columns include concentrations in dissolved organic carbon and nitrogen, concentration in nitrate and total of organic acids, as well as soil temperature and moisture at the beginning of the field experiment. Mean values are presented with their standard deviation

Country	Site name	Dissolved organic carbon content (mg C L^{-1})	Dissolved nitrogen content (mg N L^{-1})	Nitrate content (mg N L^{-1})	Total organic acids content (mg C L^{-1})	Initial soil temperature (°C)	Initial soil moisture (unitless)
Detection limit		0.01	0.1	0.01	0.002		
Belgium	Dyle Valley	45.403 ± 12.227	2.708 ± 0.309	0.079 ± 0.011	0.220 ± 0.117	16.73 ± 0.87	0.59 ± 0.03
Belgium	Zuidleie	42.053 ± 4.449	3.037 ± 0.237	0.069 ± 0.009	0.209 ± 0.046	17.15 ± 0.83	0.72 ± 0.03
Belgium	Zwarte Beek	Not measured	Not measured	Not measured	Not measured	Not measured	Not measured
Estonia	Agali	76.620 ± 11.212	30.557 ± 9.687	20.883 ± 8.341	0.157 ± 0.045	16.57 ± 0.43	0.25 ± 0.26
Estonia	Kuresoo	Not measured	Not measured	Not measured	Not measured	Not measured	Not measured
Estonia	Kuresoo Control	Not measured	Not measured	Not measured	Not measured	Not measured	Not measured
Estonia	Laiuse	81.103 ± 10.967	4.319 ± 0.827	1.480 ± 0.397	0.267 ± 0.016	24.67 ± 0.53	0.63 ± 0.08
Estonia	Laiuse Control	100.147 ± 12.972	2.996 ± 0.445	0.198 ± 0.133	0.337 ± 0.048	20.08 ± 0.13	0.60 ± 0.03
Finland	Kivalo	43.820 (no replicate)	1.611 (no replicate)	0.057 (no replicate)	0.336 (no replicate)	11.88 ± 1.26	0.44 ± 0.09
Finland	Kivalo Control	77.890 (no replicate)	2.723 (no replicate)	0.754 (no replicate)	0.360 (no replicate)	10.21 ± 0.08	0.47 ± 0.01
Finland	Lettosuo	30.900 (no replicate)	2.016 (no replicate)	0.697 ± 0.586	0.299 ± 0.232	18.42 ± 2.42	0.52 ± 0.12
Finland	Lettosuo Control	25.180 (no replicate)	5.945 (no replicate)	3.458 ± 0.546	0.194 ± 0.110	18.33 ± 2.58	0.71 ± 0.13
Finland	Rottasniitunsuo	114.300 (no replicate)	6.549 (no replicate)	0.388 ± 0.339	0.724 ± 0.898	18.71 ± 0.54	0.00 ± 0.01
France	Bernadouze	55.000 ± 11.922	2.901 ± 0.287	0.030 ± 0.033	0.513 ± 0.180	20.23 ± 0.68	0.53 ± 0.05
France	Confluent dry	23.100 (no replicate)	3.124 (no replicate)	1.242 ± 0.223	0.078 ± 0.017	19.17 ± 0.24	0.35 ± 0.01
France	Confluent wet	152.600 (no replicate)	4.310 (no replicate)	0.183 ± 0.126	0.214 ± 0.166	17.92 ± 0.23	0.58 ± 0.01
France	Rhinau	25.750 (no replicate)	2.899 (no replicate)	0.636 ± 0.206	0.084 ± 0.004	15.13 ± 0.22	0.42 ± 0.01
Spain	Canoves	32.060 ± 3.564	2.675 ± 0.428	0.170 ± 0.317	0.124 ± 0.049	16.17 ± 0.11	0.48 ± 0.02
Spain	Estanyeres	66.000 (no replicate)	5.581 (no replicate)	0.073 ± 0.017	0.363 ± 0.185	19.75 ± 0.80	0.53 ± 0.06
Spain	Rubio	22.380 ± 3.135	1.284 ± 0.176	0.059 ± 0.031	0.635 ± 0.677	16.60 ± 0.45	0.58 ± 0.04
Spain	Tordera	134.857 ± 60.661	5.463 ± 1.323	0.072 ± 0.016	0.173 ± 0.057	17.25 ± 0.38	0.53 ± 0.01

Open Access This article is licensed under a Creative Commons Attribution 4.0 International License, which permits use, sharing, adaptation, distribution and reproduction in any medium or format, as long as you give appropriate credit to the original author(s) and the source, provide a link to the Creative Commons licence, and indicate if changes were made. The images or other third party material in this article are included in the article's Creative Commons licence, unless indicated otherwise in a credit line to the material. If material is not included in the article's Creative Commons licence and your intended use is not permitted by statutory regulation or exceeds the permitted use, you will need to obtain permission directly from the copyright holder. To view a copy of this licence, visit http://creativecommons.org/licenses/by/4.0/.

References

Ackett R, Hilafu H, Gelfand I, Saha D (2025) Statistical identification of nitrous oxide hot moments and their significance across global agroecosystems. J Geophys Res Biogeosci 130(10):e2025JG008953. https://doi.org/10.1029/2025JG008953

ALFAwetlands Project (2022) Project overview. Available at: https://alfawetlands.eu/alfawetland/milestones/. Accessed 30 Oct 2025

Almaraz M, Wong MY, Yang WH (2020) Looking back to look ahead: a vision for soil denitrification research. Ecology 101(1):e02917. https://doi.org/10.1002/ecy.2917

Anthony TL, Silver WL (2021) Hot moments drive extreme nitrous oxide and methane emissions from agricultural peatlands. Glob Chang Biol 27(20):5141–5153. https://doi.org/10.1111/gcb.15802

Bahram M, Espenberg M, Pärn J, Lehtovirta-Morley L, Anslan S, Kasak K, Kõljalg U, Liira J, Maddison M, Moora M, Niinemets Ü, Öpik M, Pärtel M, Soosaar K, Zobel M, Hildebrand F, Tedersoo L, Mander Ü (2022) Structure and function of the soil microbiome underlying N_2O emissions from global wetlands. Nat Commun 13(1):1430. https://doi.org/10.1038/s41467-022-29161-3

Berger S, Jang I, Seo J, Kang H, Gebauer G (2013a) A record of N_2O and CH_4 emissions and underlying soil processes of Korean rice paddies as affected by different water management practices. Biogeochemistry 115(1–3):317–332. https://doi.org/10.1007/s10533-013-9837-1

Berger S, Jung E, Köpp J, Kang H, Gebauer G (2013b) Monsoon rains, drought periods and soil texture as drivers of soil N_2O fluxes – soil drought turns East Asian temperate deciduous forest soils into temporary and unexpectedly persistent N_2O sinks. Soil Biol Biochem 57:273–281. https://doi.org/10.1016/j.soilbio.2012.09.026

Boyer EW, Alexander RB, Parton WJ, Li C, Butterbach-Bahl K, Donner SD, Skaggs RW, Grosso SJD (2006) Modeling denitrification in terrestrial and aquatic ecosystems at regional scales. Ecol Appl 16(6):2123–2142. https://doi.org/10.1890/1051-0761(2006)016[2123:MDITAA]2.0.CO;2

Butterbach-Bahl K, Baggs EM, Dannenmann M, Kiese R, Zechmeister-Boltenstern S (2013) Nitrous oxide emissions from soils: how well do we understand the processes and their controls? Philos Trans R Soc Lond B Biol Sci 368(1621):20130122. https://doi.org/10.1098/rstb.2013.0122

Chen Z, Shi L, Ye M, Zhu Y, Yang J (2018) Global sensitivity analysis for identifying important parameters of nitrogen nitrification and denitrification under model uncertainty and scenario uncertainty. J Hydrol 561:884–895. https://doi.org/10.1016/j.jhydrol.2018.04.031

Christensen S, Rousk K (2024) Global N_2O emissions from our planet: which fluxes are affected by man, and can we reduce these? iScience 27(2):109042. https://doi.org/10.1016/j.isci.2024.109042

Congreves KA, Wagner-Riddle C, Si BC, Clough TJ (2018) Nitrous oxide emissions and biogeochemical responses to soil freezing-thawing and drying-wetting. Soil Biol Biochem 117:5–15. https://doi.org/10.1016/j.soilbio.2017.10.040

Davidson EA, Verchot LV (2000) Testing the hole-in-the-pipe model of nitric and nitrous oxide emissions from soils using the TRAGNET database. Glob Biogeochem Cycles 14(4):1035–1043. https://doi.org/10.1029/1999GB001223

De Sisto M, Somes C, Landolfi A, MacDougall AH (2024) Projecting atmospheric N_2 O rise until the end of the 21st century: an earth system model study. Environ Res Lett 19(12):124036. https://doi.org/10.1088/1748-9326/ad8c6c

Del Grosso SJ, Smith W, Kraus D, Massad RS, Vogeler I, Fuchs K (2020) Approaches and concepts of modelling denitrification: increased process understanding using observational data can reduce uncertainties. Curr Opin Environ Sustain 47:37–45. https://doi.org/10.1016/j.cosust.2020.07.003

Dinsmore KJ, Skiba UM, Billett MF, Rees RM (2008) Effect of water table on greenhouse gas emissions from peatland mesocosms. Plant Soil 318(1–2):229–242. https://doi.org/10.1007/s11104-008-9832-9

Douglas EJ, Gammal J, Needham HR, Stephenson F, Townsend M, Pilditch CA, Lohrer AM (2022) Combining techniques to conceptualise denitrification hot spots and hot moments in estuaries. Ecosystems 25(8):1670–1681. https://doi.org/10.1007/s10021-021-00732-7

Ebrahimi A, Or D (2016) Microbial community dynamics in soil aggregates shape biogeochemical gas fluxes from soil profiles – upscaling an aggregate biophysical model. Glob Change Biol 22(9):3141–3156. https://doi.org/10.1111/gcb.13345

Felber R, Conen F, Flechard CR, Neftel A (2012) Theoretical and practical limitations of the acetylene inhibition technique to determine total denitrification losses. Biogeosciences 9(10):4125–4138. https://doi.org/10.5194/bg-9-4125-2012

Friedl J, Cardenas LM, Clough TJ, Dannenmann M, Hu C, Scheer C (2020) Measuring denitrification and the N_2O:(N_2O + N_2) emission ratio from terrestrial soils. Curr Opin Environ Sustain 47:61–71. https://doi.org/10.1016/j.cosust.2020.08.006

Frostegård Å, Vick SHW, Lim NYN, Bakken LR, Shapleigh JP (2022) Linking meta-omics to the kinetics of denitrification intermediates reveals pH-dependent causes of N_2O emissions and nitrite accumulation in soil. ISME J 16(1):26–37. https://doi.org/10.1038/s41396-021-01045-2

Goldberg SD, Gebauer G (2009) Drought turns a Central European Norway spruce forest soil from an N_2 O source to a transient N_2 O sink. Glob Change Biol 15(4):850–860. https://doi.org/10.1111/j.1365-2486.2008.01752.x

Goldberg SD, Knorr K-H, Gebauer G (2008) N2 O concentration and isotope signature along profiles provide deeper insight into the fate of N_2 O in soils†. Isot Environ Health Stud 44(4):377–391. https://doi.org/10.1080/10256010802507433

Goldberg SD, Knorr K, Blodau C, Lischeid G, Gebauer G (2010) Impact of altering the water table height of an acidic fen on N_2 O and NO fluxes and soil concentrations. Glob Change Biol 16(1):220–233. https://doi.org/10.1111/j.1365-2486.2009.02015.x

Groffman PM (2012) Terrestrial denitrification: challenges and opportunities. Ecol Process 1(1):11. https://doi.org/10.1186/2192-1709-1-11

Groffman PM, Altabet MA, Böhlke JK, Butterbach-Bahl K, David MB, Firestone MK, Giblin AE, Kana TM, Nielsen LP, Voytek MA (2006) Methods for measuring denitrification: diverse approaches to a difficult problem. Ecol Appl 16(6):2091–2122. https://doi.org/10.1890/1051-0761(2006)016[2091:MFMDDA]2.0.CO;2

Groffman PM, Butterbach-Bahl K, Fulweiler RW, Gold AJ, Morse JL, Stander EK, Tague C, Tonitto C, Vidon P (2009) Challenges to incorporating spatially and temporally explicit phenomena (hotspots and hot moments) in denitrification models. Biogeochemistry 93(1–2):49–77. https://doi.org/10.1007/s10533-008-9277-5

Guilhen J, Al Bitar A, Sauvage S, Parrens M, Martinez J-M, Abril G, Moreira-Turcq P, Sánchez-Pérez J-M (2020) Denitrification and associated nitrous oxide and carbon dioxide emissions from the Amazonian wetlands. Biogeosciences 17(16):4297–4311. https://doi.org/10.5194/bg-17-4297-2020

Guo X, Drury CF, Yang X, Daniel Reynolds W, Fan R (2014) The extent of soil drying and rewetting affects nitrous oxide emissions, denitrification, and nitrogen mineralization. Soil Sci Soc Am J 78(1):194–204. https://doi.org/10.2136/sssaj2013.06.0219

Hardison AK, Algar CK, Giblin AE, Rich JJ (2015) Influence of organic carbon and nitrate loading on partitioning between dissimilatory nitrate reduction to ammonium (DNRA) and N_2 production. Geochim Cosmochim Acta 164:146–160. https://doi.org/10.1016/j.gca.2015.04.049

Heinen M (2006) Simplified denitrification models: overview and properties. Geoderma 133(3–4):444–463. https://doi.org/10.1016/j.geoderma.2005.06.010

Hénault C, Germon JC (2000) NEMIS, a predictive model of denitrification on the field scale. Eur J Soil Sci 51(2):257–270. https://doi.org/10.1046/j.1365-2389.2000.00314.x

Hernandez ME, Mitsch WJ (2006) Influence of hydrologic pulses, flooding frequency, and vegetation on nitrous oxide emissions from created riparian marshes. Wetlands 26(3):862–877. https://doi.org/10.1672/0277-5212(2006)26[862:IOHPFF]2.0.CO;2

Hernández-del Amo E, Bañeras L (2021) Effects of high nitrate input in the denitrification-DNRA activities in the sediment of a constructed wetland under varying C/N ratios. Ecol Eng 159:106098. https://doi.org/10.1016/j.ecoleng.2020.106098

Hu H-W, Chen D, He J-Z (2015) Microbial regulation of terrestrial nitrous oxide formation: understanding the biological pathways for prediction of emission rates. FEMS Microbiol Rev 39(5):729–749. https://doi.org/10.1093/femsre/fuv021

Jørgensen CJ, Elberling B (2012) Effects of flooding-induced N_2O production, consumption and emission dynamics on the annual N_2O emission budget in wetland soil. Soil Biol Biochem 53:9–17. https://doi.org/10.1016/j.soilbio.2012.05.005

Kanaan R, Darnajoux R, Escarmena L, Sauvage S, Camboulive T, Druilhe J-L, Sánchez-Pérez JM (2025) A new method to investigate denitrification dynamics during simulated floods in soils. Eur J Soil Sci 76(2):e70098. https://doi.org/10.1111/ejss.70098

Kazmi FA, Espenberg M, Pärn J, Masta M, Ranniku R, Thayamkottu S, Mander Ü (2025) Meltwater of freeze-thaw cycles drives N_2O-governing microbial communities in a drained peatland forest soil. Biol Fertil Soils 61(3):667–680. https://doi.org/10.1007/s00374-023-01790-w

Khalil K, Renault P, Guérin N, Mary B (2005) Modelling denitrification including the dynamics of denitrifiers and their progressive ability to reduce nitrous oxide: comparison with batch experiments. Eur J Soil Sci 56(4):491–504. https://doi.org/10.1111/j.1365-2389.2004.00681.x

Klionsky SM, Neill C, Helton AM, Lawrence B (2024) Groundwater seeps are hot spots of denitrification and N_2O emissions in a restored wetland. Biogeochemistry 167(8):1041–1056. https://doi.org/10.1007/s10533-024-01156-w

Knowles R (1982) Denitrification. Microbiol Rev 46(1):43–70. https://doi.org/10.1128/mr.46.1.43-70.1982

Lind LPD, Audet J, Tonderski K, Hoffmann CC (2013) Nitrate removal capacity and nitrous oxide production in soil profiles of nitrogen loaded riparian wetlands inferred by laboratory microcosms. Soil Biol Biochem 60:156–164. https://doi.org/10.1016/j.soilbio.2013.01.021

Mander Ü, Well R, Weymann D, Soosaar K, Maddison M, Kanal A, Lõhmus K, Truu J, Augustin J, Tournebize J (2014) Isotopologue ratios of N_2 O and N_2 measurements underpin the importance of denitrification in differently N-Loaded riparian alder forests. Environ Sci Technol 48(20):11910–11918. https://doi.org/10.1021/es501727h

Mander Ü, Krasnova A, Escuer-Gatius J, Espenberg M, Schindler T, Machacova K, Pärn J, Maddison M, Megonigal JP, Pihlatie M, Kasak K, Niinemets Ü, Junninen H, Soosaar K (2021) Forest canopy mitigates soil N_2O emission during hot moments. Npj Clim Atmos Sci 4(1):39. https://doi.org/10.1038/s41612-021-00194-7

Martínez-Espinosa C, Sauvage S, Al Bitar A, Green PA, Vörösmarty CJ, Sánchez-Pérez JM (2021) Denitrification in wetlands: a review towards a quantification at global scale. Sci Total Environ 754:142398. https://doi.org/10.1016/j.scitotenv.2020.142398

Martínez-Espinosa C, Sauvage S, Al Bitar A, Sánchez Pérez JM (2022) A dynamic model for assessing soil denitrification in large-scale natural wetlands driven by earth observations. Environ Model Softw 158:105557. https://doi.org/10.1016/j.envsoft.2022.105557

Masta M, Espenberg M, Gadegaonkar SS, Pärn J, Sepp H, Kirsimäe K, Sgouridis F, Müller C, Mander Ü (2022) Integrated isotope and microbiome analysis indicates dominance of denitrification in N_2O production after rewetting of drained fen peat. Biogeochemistry 161(2):119–136. https://doi.org/10.1007/s10533-022-00971-3

Masta M, Espenberg M, Kuusemets L, Pärn J, Thayamkottu S, Sepp H, Kirsimäe K, Sgouridis F, Kasak K, Soosaar K, Mander Ü (2024) 15N tracers and microbial analyses reveal in situ N_2O sources in contrasting water regimes of a drained peatland forest. Pedosphere 34(4):749–758. https://doi.org/10.1016/j.pedsph.2023.06.006

O'Connell CS, Anthony TL, Mayes MA, Pérez T, Sihi D, Silver WL (2022) Utilizing novel field and data exploration methods to explore hot moments in high-frequency soil nitrous oxide emissions data: opportunities and challenges. Front for Glob Change 5:674348. https://doi.org/10.3389/ffgc.2022.674348

ÖQuist MG, Nilsson M, Sörensson F, Kasimir-Klemedtsson Å, Persson T, Weslien P, Klemedtsson L (2004) Nitrous oxide production in a forest soil at low temperatures â€“ processes and environmental controls. FEMS Microbiol Ecol 49(3):371–378. https://doi.org/10.1016/j.femsec.2004.04.006

Or D (2020) The tyranny of small scales—on representing soil processes in global land surface models. Water Resour Res 56(6):2019WR024846. https://doi.org/10.1029/2019WR024846

Pärn J, Verhoeven JTA, Butterbach-Bahl K, Dise NB, Ullah S, Aasa A, Egorov S, Espenberg M, Järveoja J, Jauhiainen J, Kasak K, Klemedtsson L, Kull A, Laggoun-Défarge F, Lapshina ED, Lohila A, Lõhmus K, Maddison M, Mitsch WJ, Müller C, Niinemets Ü, Osborne B, Pae T, Salm J-O, Sgouridis F, Sohar K, Soosaar K, Storey K, Teemusk A, Tenywa MM, Tournebize J, Truu J, Veber G, Villa JA, Zaw SS, Mander Ü (2018) Nitrogen-rich organic soils under warm well-drained conditions are global nitrous oxide emission hotspots. Nat Commun 9(1):1135. https://doi.org/10.1038/s41467-018-03540-1

Peng B, Sun J, Liu J, Dai W, Sun L, Pei G, Gao D, Wang C, Jiang P, Bai E (2019) N_2O emission from a temperate forest soil during the freeze-thaw period: a mesocosm study. Sci Total Environ 648:350–357. https://doi.org/10.1016/j.scitotenv.2018.08.155

Peyrard D, Delmotte S, Sauvage S, Namour P, Gerino M, Vervier P, Sanchez-Perez JM (2011) Longitudinal transformation of nitrogen and carbon in the hyporheic zone of an N-rich stream: a combined modelling and field study. Phys Chem Earth Parts A B C 36(12):599–611. https://doi.org/10.1016/j.pce.2011.05.003

Powlson DS, Saffigna PG, Kragt-Cottaar M (1988) Denitrification at sub-optimal temperatures in soils from different climatic zones. Soil Biol Biochem 20(5):719–723. https://doi.org/10.1016/0038-0717(88)90157-5

Ranniku R, Mander Ü, Escuer-Gatius J, Schindler T, Kupper P, Sellin A, Soosaar K (2024) Dry and wet periods determine stem and soil greenhouse gas fluxes in a northern drained peatland forest. Sci Total Environ 928:172452. https://doi.org/10.1016/j.scitotenv.2024.172452

Ravishankara AR, Daniel JS, Portmann RW (2009) Nitrous oxide (N_2 O): the dominant ozone-depleting substance emitted in the 21st century. Science 326(5949):123–125. https://doi.org/10.1126/science.1176985

Richardson M, Amos R, Lapen D, Blowes D, Ptacek C (2025) Importance of short-term variations in greenhouse gas emission and cycling along agricultural riparian zone soils. Vadose Zone J 24(1):e70005. https://doi.org/10.1002/vzj2.70005

Scheer C, Fuchs K, Pelster DE, Butterbach-Bahl K (2020) Estimating global terrestrial denitrification from measured N_2O:(N_2O + N_2) product ratios. Curr Opin Environ Sustain 47:72–80. https://doi.org/10.1016/j.cosust.2020.07.005

Schlüter S, Lucas M, Grosz B, Ippisch O, Zawallich J, He H, Dechow R, Kraus D, Blagodatsky S, Senbayram M, Kravchenko A, Vogel H-J, Well R (2025) The anaerobic soil volume as a controlling factor of denitrification: a review. Biol Fertil Soils 61(3):343–365. https://doi.org/10.1007/s00374-024-01819-8

Schreiber F, Wunderlin P, Udert KM, Wells GF (2012) Nitric oxide and nitrous oxide turnover in natural and engineered microbial communities: Biological pathways, chemical reactions, and novel technologies. Front Microbiol. https://doi.org/10.3389/fmicb.2012.00372

Sihi D, Davidson EA, Savage KE, Liang D (2020) Simultaneous numerical representation of soil microsite production and consumption of carbon dioxide, methane, and nitrous oxide using probability distribution functions. Glob Change Biol 26(1):200–218. https://doi.org/10.1111/gcb.14855

Stuchiner ER, Xu J, Eddy WC, DeLucia EH, Yang WH (2025) Hot or not? An evaluation of methods for identifying hot moments of nitrous oxide emissions from soils. J Geophys Res Biogeosci 130(1):e2024JG008138. https://doi.org/10.1029/2024JG008138

Tian H, Pan N, Thompson RL, Canadell JG, Suntharalingam P, Regnier P, Davidson EA, Prather M, Ciais P, Muntean M, Pan S, Winiwarter W, Zaehle S, Zhou F, Jackson RB, Bange HW, Berthet S, Bian Z, Bianchi D, Bouwman AF, Buitenhuis ET, Dutton G, Hu M, Ito A, Jain AK, Jeltsch-Thömmes A, Joos F, Kou-Giesbrecht S, Krummel PB, Lan X, Landolfi A, Lauerwald R, Li Y, Lu C, Maavara T, Manizza M, Millet DB, Mühle J, Patra PK, Peters GP, Qin X, Raymond P, Resplandy L, Rosentreter JA, Shi H, Sun Q, Tonina D, Tubiello FN, van der Werf GR, Vuichard N, Wang J, Wells KC, Western LM, Wilson C, Yang J, Yao Y, You Y, Zhu Q (2024) Global nitrous oxide budget (1980–2020). Earth Syst Sci Data 16(6):2543–2604. https://doi.org/10.5194/essd-16-2543-2024

Tiedje JM, Simkins S, Groffman PM (1989) Perspectives on measurement of denitrification in the field including recommended protocols for acetylene based methods. Plant Soil. https://doi.org/10.1007/bf02202594

Tilsner J, Wrage N, Lauf J, Gebauer G (2003) Emission of gaseous nitrogen oxides from an extensively managed grassland in NE Bavaria, Germany. Biogeochemistry 63:249–267. https://doi.org/10.1023/A:1023316315550

van den Berg EM, Boleij M, Kuenen JG, Kleerebezem R, Van Loosdrecht MCM (2016) DNRA and denitrification coexist over a broad range of acetate/N-NO_3^- ratios, in a chemostat enrichment culture. Front Microbiol. https://doi.org/10.3389/fmicb.2016.01842

van den Heuvel RN, Hefting MM, Tan NCG, Jetten MSM, Verhoeven JTA (2009) N_2O emission hotspots at different spatial scales and governing factors for small scale hotspots. Sci Total Environ 407(7):2325–2332. https://doi.org/10.1016/j.scitotenv.2008.11.010

Vidon P, Marchese S, Welsh M, McMillan S (2016) Impact of precipitation intensity and riparian geomorphic characteristics on greenhouse gas emissions at the soil-atmosphere interface in a water-limited riparian zone. Water Air Soil Pollut 227(1):8. https://doi.org/10.1007/s11270-015-2717-7

Wagner-Riddle C, Congreves KA, Abalos D, Berg AA, Brown SE, Ambadan JT, Gao X, Tenuta M (2017) Globally important nitrous oxide emissions from croplands induced by freeze–thaw cycles. Nat Geosci 10(4):279–283. https://doi.org/10.1038/ngeo2907

Wallenstein MD, Vilgalys RJ (2005) Quantitative analyses of nitrogen cycling genes in soils. Pedobiologia 49(6):665–672. https://doi.org/10.1016/j.pedobi.2005.05.005

Wang B, Brewer PE, Shugart HH, Lerdau MT, Allison SD (2019) Soil aggregates as biogeochemical reactors and implications for soil–atmosphere exchange of greenhouse gases—a concept. Glob Change Biol 25(2):373–385. https://doi.org/10.1111/gcb.14515

Weier KL, Doran JW, Power JF, Walters DT (1993) Denitrification and the dinitrogen/nitrous oxide ratio as affected by soil water, available carbon, and nitrate. Soil Sci Soc Am J 57(1):66–72. https://doi.org/10.2136/sssaj1993.03615995005700010013x

Wild J, Kopecký M, Macek M, Šanda M, Jankovec J, Haase T (2019) Climate at ecologically relevant scales: a new temperature and soil moisture logger for long-term microclimate measurement. Agric for Meteorol 268:40–47. https://doi.org/10.1016/j.agrformet.2018.12.018

Wrage N, Lauf J, Del Prado A, Pinto M, Pietrzak S, Yamulki S, Oenema O, Gebauer G (2004) Distinguishing sources of N_2 O in European grasslands by stable isotope analysis. Rapid Commun Mass Spectrom 18(11):1201–1207. https://doi.org/10.1002/rcm.1461

Xu Z, Hattori S, Masuda Y, Toyoda S, Koba K, Yu P, Yoshida N, Du Z-J, Senoo K (2024) Unprecedented N_2 O production by nitrate-ammonifying Geobacteraceae with distinctive N_2 O isotopocule signatures. Mbio 15(12):e02540-24. https://doi.org/10.1128/mbio.02540-24

Zhao S, Zhang B, Sun X, Yang L (2021) Hot spots and hot moments of nitrogen removal from hyporheic and riparian zones: a review. Sci Total Environ 762:144168. https://doi.org/10.1016/j.scitotenv.2020.144168

Publisher's Note Springer Nature remains neutral with regard to jurisdictional claims in published maps and institutional affiliations.